Electronic Supplementary Material (ESI) for Chemical Science.

A series of caged fluorophores for calibrating light intensity

Mrinal Mandal,[a] Hessam Sepasi Tehrani,[a] Qianhua Mai,[a] Emma Simon,[a] Marie-Aude Plamont,[a] Christine Rampon,[b] Sophie Vriz,[b] Isabelle Aujard,[a,*] Thomas Le Saux,[a,*] Ludovic Jullien[a,*]

[a] PASTEUR, Département de chimie, École normale supérieure, PSL University, Sorbonne Université, CNRS, 24, rue Lhomond, 75005 Paris, France.

[b] Laboratoire des biomolécules (LBM), Département de chimie, École normale supérieure, PSL University, Sorbonne Université, CNRS, 24, rue Lhomond, 75005 Paris, France.

∗To whom correspondence should be addressed; E-mail:

Isabelle.Aujard@ens.psl.eu,

Thomas.Lesaux@ens.psl.eu,

Ludovic.Jullien@ens.psl.eu.

Table of Contents

Experimental section

General information

4,5-dimethoxy-2-nitrobenzyl bromide and trisodium 8-hydroxypyrene-1,3,6-trisulfonate were purchased from Acros Organics. Commercially available reagents were used as obtained. ^{1}H, ^{13}C, and ^{19}F NMR spectra were recorded at 300 K on a Bruker AM 300 spectrometer; chemical shifts are reported in ppm with protonated solvent as internal reference (^{1}H, $CHCl_3$ in $CDCl_3$ 7.26 ppm, CHD_2SOCD_3 in CD_3SOCD_3 2.50 ppm, CHD_2COCD_3 in CD_3COCD_3 2.05 ppm; ^{13}C, $^{13}CDCl_3$ in $CDCl_3$ 77.0 ppm, $^{13}CD_3SOCD_3$ in CD_3SOCD_3 39.5 ppm, $^{13}CD_3COCD_3$ in CD_3COCD_3 29.9 ppm; ^{19}F, $C_7H_5F_3$ in CHD_2SOCD_3 -63.7 ppm). Mass spectra (chemical ionization and electronic impact with NH_3 or CH_4) were performed by the Service de Spectrométrie de Masse de Chimie ParisTech and mass spectra high resolution were performed by the Service de Spectrométrie de Masse de l'Institut de Chimie Organique et Analytique (Orléans). Column chromatography was performed on silica gel 60 (0.040–0.063 nm; Merck). Analytical thin-layer chromatography (TLC) was conducted on Merck silica gel 60 F254 pre-coated plates.

Synthesis procedures

Trisodium 8-(4,5-dimethoxy-2-nitrobenzyloxy)pyrene -1,3,6-trisulfonic acid NPy-S

Potassium carbonate (0.17 g, 1.2 mmol, 1.2 eq.), tetrabutyl ammonium chloride (0.89 g, 3.2 mmol, 3.2 eq.) and 4,5-dimethoxy-2-nitrobenzyl bromide (0.33 g, 1.2 mmol, 1.2 eq.) were added to trisodium 8-hydroxypyrene-1,3,6-trisulfonic acid (**HPTS**, 0.52 g, 1 mmol) suspended in acetonitrile (20 mL). The resulting reaction mixture was then refluxed for 24 h in the dark. After the suspension was cooled down to room temperature, acetonitrile was removed under reduced pressure. The residue was washed with dichloromethane (5×15 mL) and dried under vacuum, yielding **NPy-S** as a light yellow powder (0.65 g, 90 %).

^{1}H-NMR (300 MHz, DMSO-d_6): δ 9.15 (1H, d, J = 10 Hz), 9.06, (1H, d, J = 10 Hz), 9.04 (1H, s), 8.97 (1H, d, J = 10 Hz), 8.40 (1H, d, J = 10 Hz), 8.33 (1H, s), 7.80 (1H, s), 7.68 (1H, s), 5.82 (2H, s), 3.99 (3H, s), 3.92 (3H, s).
^{13}C NMR (75 MHz, DMSO-d_6): δ 153.2, 150.6, 147.9, 143.2, 140.1, 139.8, 139.7, 127.8, 127.5, 127.2, 126.3, 126.2, 125.5, 125.0, 124.4, 123.9, 120.9, 119.8, 119.7, 111.3, 109.2, 108.4, 67.5, 56.2, 56.1.
HRMS (ESI): m/z calc. for $C_{25}H_{16}NNa_2O_{14}S_3$: 695.953379, found: 695.952248 $[M\text{-}Na]^-$.

Trisodium 8-(4-(oxymethyl)-6,7-dimethoxy-2H-chromen-2-one)pyrene-1,3,6-trisulfonic acid CPy-S

Potassium carbonate (39 mg, 0.29 mmol, 1.5 eq.) and 6,7-dimethoxy-4-bromomethyl coumarin (86 mg, 0.29 mmol, 1.5 eq.) were added to trisodium 8-hydroxypyrene-1,3,6-trisulfonic acid (**HPTS**, 100 mg, 0.19 mmol) in acetonitrile/H_2O (v/v, 9/3, 12 mL). The resulting reaction mixture was then heated at 80°C for 24 h in the dark. After cooling to room temperature, the precipitate was filtered, washed with acetonitrile/H_2O (v/v, 9/1) and finally with dichloromethane and dried *in vacuo* over P_2O_5. The pure compound **CPy-S** was obtained as a light yellow powder (105 mg, 74 %).

^{1}H-NMR (300 MHz, DMSO-d_6): δ 9.16 (1H, d, J = 9 Hz), 9.05, (1H, d, J = 9 Hz), 9.02 (1H, s), 8.98 (1H, d, J = 9 Hz), 8.43 (1H, d, J = 9 Hz), 8.35 (1H, s), 7.39 (1H, s), 7.17 (1H, s), 6.06 (s,1H), 5.85 (2H, s), 3.90 (3H, s), 3.80 (3H, s).
^{13}C NMR (75 MHz, DMSO-d_6): δ 160.4, 152.8, 151.5, 150.4, 149.2, 145.9, 143.3, 140.2, 139.9, 127.8, 127.5, 126.4, 126.2, 125.5, 125.1, 124.5, 124.1, 121.2, 119.9, 119.9, 109.7 (2C), 109.4, 106.0, 100.4, 66.9, 56.2, 56.0
HRMS (ESI): m/z calc. for $C_{28}H_{19}O_{14}S_3$: 674.9942, found: 674.9936 $[M\text{-}H]^-$.

Trisodium 8-acetoxypyrene-1,3,6-trisulfonic acid 1[1]

Trisodium 8-hydroxypyrene-1,3,6-trisulfonic acid (HPTS, 2.28 g, 4.35 mmol) and sodium acetate (35.7 mg, 0.44 mmol) were suspended in acetic anhydride (25 mL) and refluxed for 35 h. After the suspension was cooled down to room temperature, it was diluted with THF and filtered off. The residue was washed with acetone and dried under vacuum, yielding a grey powder (2.26 g, 92%).

^{1}H NMR (300 MHz, DMSO-d_6): δ 9.23 (1H, d, J = 10 Hz), 9.15 (1H, d, J = 10 Hz), 9.10 (1H, d, J = 10 Hz), 9.07 (1H, s), 8.26 (1H, s), 8.11 (1H, d, J = 10 Hz), 2.56 (3H, s).

8-Acetoxypyrene-1,3,6-trisulfonyl chloride 2

The compound **1** (1.0 g, 1.8 mmol) was suspended in anhydrous dichloromethane (80 mL). Oxalyl chloride (1.35 mL, 16 mmol, 9 eq) was added followed by 10 drops of anhydrous dimethylformamide. The resulting mixture was stirred at room temperature under inert atmosphere for 18 h. The solvent was evaporated. The crude was dissolved in anhydrous dichloromethane (3x20 mL) and then the solution was concentrated under reduced pressure. Compound **2** was obtained as a yellow/orange powder and used without further purification for the next step.

8-Hydroxypyrene-N',N'',N'''-trishydroxyethyl-1,3,6-trisulfonamide Py-Aa

Compound **2** (0.140 g, 0.25 mmol) was dissolved in anhydrous dichloromethane (10 mL). The solution was then cooled to 0 °C and a solution of ethanolamine (0.137 g, 2.25 mmol, 9 eq.) in anhydrous dichloromethane (5 mL) was added dropwise. The reaction mixture was stirred under inert atmosphere for 48 h at room temperature, yielding a red precipitate. The crude residue was purified by flash chromatography using acetone/cyclohexane (75/25 v/v) as eluent. The pure product was further recrystallized using acetone/pentane (70/30 v/v), yielding **Py-Aa** as orange powder (70 mg, 48 % yield).

^{1}H-NMR (300 MHz, acetone-d_6): δ 9.36 (1H, s), 9.29 (1H, d, J = 10 Hz), 9.20 (1H, d, J = 10 Hz), 9.06 (1H, d, J = 10 Hz), 8.86 (1H, d, J = 10 Hz), 8.50 (1H, s), 7.12 (3H, m) 3.50 (6H, m), 3.12 (6H, m).
^{13}C-NMR (75 MHz, DMSO-d6): δ 157.1, 137.9, 131.6, 130.4 (2C), 130.2, 128.1, 127.9, 126.0, 125.9, 125.8, 122.5, 120.5, 120.3, 117.2, 116.2, 59.9 (2C), 59.8, 45.0, 44.9 (2C).
HRMS (ESI): m/z calc. for $C_{22}H_{26}N_3O_{10}S_3$: 588.077483, found: 588.078556 $[M+H]^+$.

8-Hydroxypyrene-N',N'',N'''-tris-N-methylpiperazine-1,3,6-trisulfonamide Py-Ab

Compound **2** (1.0 g, 1.8 mmol) was dissolved in anhydrous dichloromethane (25 mL). The solution was then cooled to 0°C before the addition of N-methylpiperazine (3.60 mL, 32 mmol, 18 eq.). The reaction mixture was stirred under inert atmosphere for 48 h at room temperature. Then dichloromethane was evaporated under vacuum. The crude mixture was then washed with cyclohexane (3x20 mL) to remove the excess of N-methylpiperazine. The crude residue was purified by recrystallization in absolute ethanol/n-pentane (70/30 v/v), yielding **Py-Ab** as a red/orange powder (760 mg, 60 % yield).

^{1}H-NMR (300 MHz, DMSO-d_6): δ 9.18 (1H, d, J = 10 Hz), 8.98 (1H, s), 8.97 (1H, d, J = 10 Hz), 8.87 (1H, d, J = 10 Hz), 8.81 (1H, d, J = 10 Hz), 8.23 (1H, s), 3.19 (8H, m), 3.07 (4H, m), 2.36 (8H, m), 2.26 (4H, m), 2.12 (6H, s), 2.04 (3H, s).
^{13}C NMR (75 MHz, DMSO-d_6): δ 158.3, 134.2, 133.1, 131.8, 130.3, 128.6, 127.0, 126.6, 126.4, 126.3, 125.9, 122.6, 121.2, 120.2, 117.7, 117.6, 53.6 (4C), 53.50 (2C), 45.1 (4C), 45.0 (2C), 44.9 (3C).
HRMS (ESI): m/z calc. for $C_{31}H_{41}N_6O_7S_3$: 705.219337, found: 705.219684 $[M+H]^+$.

8-Hydroxypyrene-N,N,N',N',N'',N''-hexamethyl-1,3,6-trisulfonamide Py-Ac[1]

Compound **2** (1.0 g, 1.8 mmol) was dissolved in anhydrous dichloromethane (25 mL). The solution was then cooled to 0°C before the addition of dimethylamine (2 M in THF, 9 mL, 32 mmol, 18 eq.). The reaction mixture was stirred under inert atmosphere for 48 h at room temperature. Then

dichloromethane was evaporated under vacuum and 1 M hydrochloric acid (10 mL) was added. The aqueous phase was extracted with dichloromethane (3×25 mL). The combined organic phases were dried over sodium sulfate and evaporated under reduced pressure. The crude residue was purified by recrystallization in absolute ethanol/n-pentane (70/30 v/v), yielding **Py-Ac** as a bright yellow powder (630 mg, 65 % yield).

^{1}H NMR (300 MHz, DMSO-d_6): δ 9.27 (1H, d, J = 10 Hz), 9.15 (1H, d, J = 10 Hz), 9.02 (1H, d, J = 10 Hz), 8.98 (1H, s), 8.87 (1H, d, J = 10 Hz), 8.30 (1H, s), 2.83 (6H, s), 2.81 (12H, s).
^{13}C NMR (300 MHz, DMSO-d_6): δ 154.6, 133.7, 132.6, 131.5, 129.8, 128.3, 128.0, 127.8, 126.1, 125.9, 125.5, 123.8, 121.6, 120.6, 119.5, 116.0, 37.3 (2C), 37.2 (4C).
MS (CI): m/z calc. for $C_{22}H_{25}N_3O_7S_3$: 539.09, found: 540.33 $[M+H]^+$.

8-Hydroxypyrene-N',N'',N'''-tris-piperidine-1,3,6-trisulfonamide Py-Ad

Compound **2** (1.0 g, 1.8 mmol) was dissolved in anhydrous dichloromethane (25 mL). The solution was then cooled to 0 °C before the addition of piperidine (3.20 mL, 32 mmol, 18 eq.). The reaction mixture was stirred under inert atmosphere for 48 h at room temperature. Then dichloromethane was evaporated under vacuum and 1 M hydrochloric acid (20 mL) was added. The aqueous phase was extracted with dichloromethane (3×25 mL). The combined organic phases were dried over sodium sulfate and evaporated under reduced pressure. The crude residue was then washed with cyclohexane/ absolute ethanol (7/3 v/v; 3×15 mL), yielding **Py-Ad** as a bright yellow powder (840 mg, 71 % yield).

^{1}H NMR (300 MHz, DMSO-d_6): δ 9.27 (1H, d, J = 10 Hz), 9.12 (1H, d, J = 10 Hz), 9.03 (1H, s), 8.99 (1H, d, J = 10 Hz), 8.86 (1H, d, J = 10 Hz), 8.33 (1H, s), 3.16 (12H, m), 1.50 (12H, m), 1.36 (6H, m).
^{13}C NMR (75 MHz, DMSO-d_6): δ 154.8, 134.4, 132.4, 131.2, 129.8, 128.7, 128.4, 128.3, 126.1, 125.9, 125.5, 123.7, 121.5, 120.7, 119.3, 116.1, 46.2 (2C), 46.1 (4C), 24.9 (6C), 22.7 (3C).
HRMS (ESI): m/z calc. for $C_{31}H_{38}N_3O_7S_3$: 660.186640, found: 660.187152 $[M+H]^+$.

8-(4,5-Dimethoxy-2-nitrobenzyloxy)pyrene-N',N'',N'''-trishydroxyethyl-1,3,6-trisulfonamide NPy-Aa

Potassium carbonate (0.023 g, 0.17 mmol, 1.2 eq.) and 4,5-dimethoxy-2-nitrobenzyl bromide (0.05 g, 0.17 mmol, 1.2 eq.) were added to a solution of compound **Py-Aa** (0.08 g, 0.14 mmol) in acetonitrile (10 mL). The reaction mixture was then heated to reflux and stirred for 24 h in the dark. The obtained precipitate was washed with dichloromethane (3×10 mL) followed by acetone (3×10 mL). The precipitate was filtered and dried under a vacuum pump, yielding **NPy-Aa** as a muted red powder (0.079 g, 73 % yield).

^{1}H-NMR (300 MHz, DMSO-d6): δ 9.26 (1H, d, J = 10 Hz), 9.16 (1H, d, J = 10 Hz), 9.14 (1H, s), 9.03 (1H, d, J = 10 Hz), 8.75 (1H, d, J = 10 Hz), 8.50 (1H, s), 7.79 (1H, s), 7.62 (1H, s), 5.97 (2H, s), 3.96 (3H, s), 3.92 (3H, s), 3.29 (6H, m), 2.91 (6H, m).
^{13}C NMR (75 MHz, DMSO-d6): δ 153.1, 153.0, 148.3, 140.1, 137.9, 132.8, 132.7, 130.5, 129.9, 127.9, 127.6, 125.8, 125.3, 125.0, 124.8, 124.4, 122.7, 121.6, 120.3, 112.1, 112.0, 108.5, 68.4, 59.9 (3C), 56.3, 56.2, 45.2 (3C).
HRMS (ESI): m/z calc. for $C_{31}H_{35}N_4O_{14}S_3$: 783.130614, found: 783.129715 $[M+H]^+$.

8-(4,5-Dimethoxy-2-nitrobenzyloxy)pyrene-N',N'',N'''-tris-N-methylpiperizine-1,3,6-trisulfonamide NPy-Ab

Potassium carbonate (0.017 g, 0.12 mmol, 1.2 eq.) and 4,5-dimethoxy-2-nitrobenzyl bromide (0.033 g, 0.12 mmol, 1.2 eq.) were added to a solution of compound **Py-Ab** (0.07 g, 0.10 mmol) in acetonitrile (10 mL). The reaction mixture was heated to reflux and stirred for 24 h in the dark. After cooling, the reaction mixture was poured into water and extracted with dichloromethane (3×25 mL). The combined

organic phases were dried over sodium sulfate and evaporated under reduced pressure. The crude residue was then purified by recrystallization in dichloromethane/n-pentane (50/50 v/v), yielding pure **NPy-Ab** as a dark red powder (49 mg, 54 % yield).

^{1}H-NMR (300 MHz, $CDCl_3$): δ 9.32 (1H, d, J= 10 Hz), 9.29 (1H, d, J = 10 Hz), 9.25 (1H, s), 9.15 (1H, d, J = 10 Hz), 8.86 (1H, d, J = 10 Hz), 8.39 (1H, s), 7.83 (1H, s), 7.35 (1H, s), 5.96 (2H, s), 4.01 (3H, s), 3.98 (3H, s), 3.28 (8H, m), 3.19 (4H, m), 2.44 (12H, m), 2.22 (6H, s), 2.21 (3H, s).
^{13}C NMR (75 MHz, $CDCl_3$,): δ 153.9, 153.3, 148.8, 140.0, 133.7, 132.5, 131.9, 130.6, 129.8, 129.7, 128.3, 126.4, 126.2, 125.8, 125.5, 125.1, 123.4, 123.2, 122.3, 113.2, 110.5, 108.6, 69.1, 56.6, 56.5, 54.2 (4C), 54.1 (2C), 45.8 (2C), 45.7 (4C), 45.7 (2C), 45.6.
HRMS (ESI): m/z calc. for $C_{40}H_{50}N_7O_{11}S_3$: 900.272495, found: 900.271354 $[M+H]^+$.

8-((4,5-Dimethoxy-2-nitrobenzyl)oxy)pyrene-N,N,N',N'',N''-hexamethyl-1,3,6-trisulfonamide NPy-Ac

Potassium carbonate (0.15 g, 1.1 mmol, 1.2 eq.) and 4,5-dimethoxy-2-nitrobenzyl bromide (0.30 g, 1.1 mmol, 1.2 eq.) were added to a solution of compound **Py-Ac** (0.50 g, 0.92 mmol) in acetonitrile (10 mL). The reaction mixture was heated to reflux and stirred for 24 h in the dark. After cooling, the precipitate was filtered and washed with acetone, yielding pure **NPy-Ac** as yellow powder (0.54 g, 79 % yield).

^{1}H-NMR (300 MHz, $CDCl_3$): δ 9.32 (1H, d, J = 10 Hz), 9.30 (1H, d, J = 10 Hz), 9.17 (1H, S), 9.14 (1H, d, J = 10 Hz), 8.86 (1H, d, J = 10 Hz), 8.41 (1H, s), 7.83 (1H, s), 7.37 (1H, s), 5.95 (2H, s), 4.02 (3H, s), 4.00 (3H, s), 2.94 (12H, s), 2.87 (6H, s).
^{13}C NMR (75 MHz, $CDCl_3$): δ 153.9, 153.3, 148.8, 140.1, 134.1, 132.6, 131.9, 130.2, 129.8, 128.4, 126.4, 126.4, 125.9, 125.5, 125.1, 123.5, 123.2, 122.4, 113.1, 112.8, 110.7, 108.6, 69.1, 56.6, 56.5, 37.7 (2C), 37.6 (2C), 37.5 (2C).
HRMS (ESI): m/z calc. for $C_{31}H_{35}N_4O_{11}S_3$: 735.145897, found: 735.145803 $[M+H]^+$.

8-(4,5-Dimethoxy-2-nitrobenzyloxy)pyrene-N',N'',N'''-tris-piperidine-1,3,6-trisulfonamide NPy-Ad

Potassium carbonate (0.025 g, 0.18 mmol, 1.2 eq.) and 4,5-dimethoxy-2-nitrobenzyl bromide (0.05 g, 0.18 mmol, 1.2 eq.) were added to a solution of compound **Py-Ad** (0.10 g, 0.15 mmol) in acetonitrile (10 mL). The reaction mixture was heated to reflux and stirred for 24 h in the dark. After cooling, the reaction mixture was poured into water and extracted with dichloromethane (3×25 mL). The combined organic phases were dried over sodium sulfate and evaporated under reduced pressure. The crude residue was then purified by flash chromatography using cyclohexane/ethyl acetate (70/30 v/v) as eluent, yielding **NPy-Ad** as a light yellow powder (80 mg, 62 % yield). [**Path a**]

8-(4,5-Dimethoxy-2-nitrobenzyloxy)pyrene -1,3,6-trisulfonyl chloride 3

The compound **NPy-S** (0.10 g, 0.14 mmol) was suspended in anhydrous dichloromethane (10 mL). Oxalyl chloride (0.11 mL, 1.3 mmol, 9 eq) was added followed by 7 drops of anhydrous dimethylformamide. The resulting mixture was stirred at room temperature in the dark and under inert atmosphere for 18 h. The solvent was evaporated. The crude residue was dissolved in anhydrous dichloromethane (3x10 mL) and then the solution was concentrated under reduced pressure. Compound **3** was obtained as a yellow/orange powder and used without further purification for the next step.

8-(4,5-Dimethoxy-2-nitrobenzyloxy)pyrene-N',N'',N'''-tris-piperidine-1,3,6-trisulfonamide NPy-Ad

Compound **3** (0.10 g, 0.14 mmol) was dissolved in anhydrous dichloromethane (10 mL). The solution was then cooled to 0 °C before the addition of piperidine (0.12 mL, 1.3 mmol, 9 eq.). The reaction mixture was stirred in the dark and under inert atmosphere for 48 h at room temperature. Then the

reaction mixture was filtered and the filtrate was evaporated under reduced pressure. The crude residue was then washed with cyclohexane/ absolute ethanol (7/3 v/v; 3×10 mL), yielding **NPy-Ad** as a bright yellow powder (60 mg, 50 % yield). [**Path b**]

^{1}H-NMR (300 MHz, $CDCl_3$): δ 9.30 (1H, d, J= 10 Hz), 9.29 (1H, d, J = 10 Hz), 9.22 (1H, s), 9.13 (1H, d, J = 10 Hz), 8.85 (1H, d, J = 10 Hz), 8.39 (1H, s), 7.83 (1H, s), 7.36 (1H, s), 5.95 (2H, s), 4.01 (3H, s), 3.98 (3H, s), 3.27 (8H, m), 3.17 (4H, m), 1.62 (12H, m) 1.47 (6H, m).
^{13}C NMR (75 MHz, $CDCl_3$): δ 153.8, 153.2, 148.8, 140.1, 134.6, 132.3, 131.7, 130.7, 130.6, 130.1, 128.2, 126.5, 126.3, 125.9, 125.5, 124.9, 123.5, 123.1, 122.2, 113.0, 110.6, 108.6, 69.1, 56.6, 56.5, 46.7 (4C), 46.6 (2C), 25.4 (4C), 25.3 (2C), 23.5 (2C), 23.4.
HRMS (ESI): m/z calc. for $C_{40}H_{47}N_4O_{11}S_3$: 855.239798, found: 855.239384 $[M+H]^+$.

Preparation and storage of the solutions

The stock solutions of the free and caged pyranines were first produced at 5-10 mM concentration in spectroscopy grade dimethyl sulfoxide (DMSO) and stored in a vial covered with aluminum foil at –20°C.

They were subsequently diluted to the final concentrations either in 10 mM pH = 7.4 PBS buffer (for **NPy-Aa-b**), 10 mM pH = 8.4 Trizma buffer (for **NPy-S** and **CPy-S**), or 1 mM pH = 8.4 Trizma buffer/acetonitrile 1/19 (v/v) for (**NPy-Ac-d**) just prior use. The resulting solutions have been covered with aluminum foil and preserved in the dark for the duration of experiment.

To determine the proton exchange constants of the free pyranine derivatives **Py-Aa** and **Py-Ab**, we used 2 μM solutions in 10 mM universal buffer prepared as follows: To 100 mL of Milli-Q water were dissolved 82 mg of sodium acetate (CH_3COONa), 120 mg of sodium dihydrogenophosphate (NaH_2PO_4) and 518.2 mg of 2-(cyclohexylamino)ethane-1-sulfonic acid (CHES). The pH of the initial solution (5.90) was then adjusted to pH = 9 with 1 M NaOH.

Preparation of the biological samples

Cells

HeLa cells (**ATCC CCL2**) and HEK 293 T cells (**ATCC CRL3216**) were cultured in Dulbecco's Modified Eagle Medium (DMEM High glucose, Hyclone, Cytiva) supplemented with phenol red and 10% (vol/vol) fetal calf serum at 37 °C in a 5% CO_2 atmosphere. For imaging, cells were seeded (3.8×10^5 cells/mL) in μ-Dish 35 mm Imaging Chamber IBIDI (Biovalley, Clinisciences) coated with poly-L-lysine (ref P4832-Sigma-Merck). After 24h, live cells were washed with DPBS (Dulbecco's Phosphate-Buffered Saline), and treated with DMEM media (without serum and phenol red). The caged pyranine derivatives **NPy-Aa-b** and **Py-Ab** were solubilized at 5 mM in DMSO then diluted in DMEM media (without serum and phenol red). The cells were then treated with fresh solution of DMEM media (without serum and phenol red) containing **NPy-Aa; NPy-Ab or Py-Ab**. After incubation for 30 min in the dark, the cells were washed with plain DMEM media (without serum and phenol red) and treated with fresh DMEM media for confocal microscope and with DPBS for epifluorescence microscope prior to illumination to avoid any possible interference, which could originate from photoreleasing the free fluorophore in the incubating solution or auto fluorescence signal from the media.

Zebrafish embryos

The caged pyranine derivative **NPy-Ab** was solubilized at 10 mM in DMSO then diluted in water. For confocal microscopic imaging, the embryos were washed with water, and treated with the **NPy-Ab** water solution at 5 hpf. After incubation for overnight in the dark, the embryos were washed with plain water prior to illumination to avoid any possible interference, which could originate from photoreleasing the free fluorophore from the surface of the embryos.

Instruments

UV/Vis absorption and fluorescence spectrometers

UV/Vis absorption spectra were recorded on a UV/Vis spectrophotometer (Cary 300 UV-Vis, Agilent Technologies, Santa Clara, CA) at 293 K equipped with a Peltier 1×1 thermostatic cell holder (Agilent Technologies). Samples were contained either in 1 cm × 1 cm (3 mL; the cuvette content was stirred) or in 0.3 cm × 0.3 cm (54 µL; the cuvette content was not stirred) quartz cuvettes (Hellma Optics, Jena, Germany). Fluorescence measurements were acquired on a LPS 220 spectrofluorometer (PTI, Monmouth Junction, NJ), equipped with a TLC50 cuvette holder (Quantum Northwest, Liberty Lake, WA) thermoregulated at 293 K.

Photochemical experiments

Light sources: In order to photoconvert the reactants and track the evolution of fluorescent products via absorbance and fluorescence under time constant illumination, the following light sources were used: (i) For the photoconversion under various light intensities with one-photon excitation, a 365 nm Light Emitting Diode (NCSU033B, Nichia Corp., Anan, Japan) monochromatically filtered (ZET 365-20, Chroma technology, Bellows Falls, VT) to generate a spatially homogeneous source of illumination; (ii) The Xenon lamp of the LPS 220 spectrofluorometer (PTI, Monmouth Junction, NJ) for photoconversion experiments at various wavelengths with one-photon excitation. In (i) and (ii), the light intensity delivered from the light sources has been calibrated by using *α*-(4-diethylamino)phenyl)-N-phenylnitrone as an actinometer[2] and rhodamine B as a fluorescent reporter[3]; (iii) For the irradiation experiments with two-photon excitation, illumination comes from a mode-locked titanium-sapphire laser (Mira pumped by Verdi, Coherent) through a 60×, 1.2 NA objective (Olympus, Japan) applied to the sample at 3 µM concentration contained in 10 mM pH = 8.4 Trizma buffer with input laser power measured after the objective with a PM100A powermeter equipped with S170C sensor (Thorlabs, NJ).

Microscopies

Epifluorescence microscope. The images of the living cells have been collected with a home-built inverted epifluorescence microscope. To illuminate the samples, the light from high power LED (NSCU033B, Nichia Corp, Japan is collimated by high-NA condensers (ACL25416U-A, *f*=16 mm, Thorlabs, NJ) and filtered by band pass filter (ET365/40; Chroma Technology, VT). The quasi-parallel beam is focused with *f*=150 mm lens (AC254-150-A Thorlabs, NJ) at the back focal plane of a 40× imaging objective (Olympus, NA = 0.75) after being reflected by a dichroic mirror (Di-FF506, Semrock, US). The LED is powered by a LED driver (LEDD1B, Thorlabs, NJ). Fluorescence emission was collected with the imaging objective, filtered by a band pass filter (FF01-525/30 Semrock, NY) before being refocused onto the sensor of an EMCCD camera (Ixon 897, Andor, Northern Ireland).

Confocal microscopy. The confocal micrographs were acquired on a Zeiss LSM 710 Laser Scanning Microscope equipped with continuous laser line at 405 nm and a Plan NeoFluar 20×/0.5 objective. ZEN software from Zeiss was used to control the microscope and collect the data. The images were analyzed with ZEN 3.6 (blue edition) software.

Data processing

The time evolution of the recorded signal *S(t)* (absorbance and fluorescence emission) has been processed either with

- a monoexponential function

$$S(t) = S(\infty) + Ae^{-\frac{t}{\tau}} \quad \text{(S1)}$$

- or a biexponential function

$$S(t) = S(\infty) + A_1 e^{-\frac{t}{\tau_1}} + A_2 e^{-\frac{t}{\tau_2}} \quad \text{(S2)}$$

Throughout the manuscript, the error bars originate from applying these fits only.

HPLC

3 mL of a solution of the caged pyranine (**NPy-Aa** and **NPy-Ab**: 2 μM in 10 mM pH = 7.4 PBS; **NPy-Ad**: 2 μM in 1 mM pH = 7.4 PBS/acetonitrile 1/19 (v/v); **NPy-S:** 2 μM in 10 mM pH = 8.4 Trizma buffer and **CPy-S:** 5 μM in 10 mM pH = 8.4 Trizma buffer were placed in a quartz cuvette (10x10 mm) and submitted to irradiation at 365 nm under stirring. Aliquots of 30 μL were drawn at regular intervals and were subsequently analyzed by high-pressure liquid chromatography using an Agilent 1260 Infinity LC System equipped with autosampler and diode array detector. Chromatographic separations were carried out by using an Atlantis T3 (for **NPy-Aa-d**) (3x150 mm, particle size 3 μm; Waters Corporation, Milford, MA) and C18 column (for **NPy-S** and **CPy-S**) (4.6x50 mm, particle size 2.7 μm; Poroshell 120) operating at 0.7 mL/min (for **NPy-Aa-d**) and 1.5 mL/min (for **NPy-S** and **CPy-S**) and thermostated at 25°C. Detection of the caged and uncaged pyranines was performed at 405 and 480 nm respectively. 15 μL (for **NPy-Aa-d**, **NPy-S**, and **CPy-S**), 25 μL (for **NPy-Ab**) were injected in the chromatographic system. The compounds **NPy-Aa-d** were eluted with a mobile phase composed of two solvents A (methanol) and B (ammonium acetate buffer, pH 5.5) whereas **NPy-S** was eluted with two solvents C (5 mM tetrabutylammonium chloride in methanol), D (5 mM tetrabutylammonium chloride and 5 mM ammonium acetate in H_2O, pH 5.5) and **CPy-S** was eluted with two solvents A (methanol) and E (10 mM triethylamine in H_2O, pH 5.5 was adjusted with glacial acetic acid). A gradient was used to optimize the separation of the analytes.

For **NPy-Aa**, the gradient used was as follow: Initially, the column was equilibrated with a mobile phase consisting of 45% A and 55% B. Six minutes after the injection, the proportion of A was linearly increased to 95 % and for one additional minute to 98%. After this step, composition of the mobile phase was set to initial condition within 0.5 min and the column was equilibrated for 9.5 min prior to next injection. Retention times for the caged (**NPy-Aa**) and free pyranine (**Py-Aa**) were t_R = 6 min and t_R = 2.3 min respectively in these experimental conditions.

For **NPy-Ab**, the gradient used was as follow: Initially, the column was equilibrated with a mobile phase consisting of 70% A and 30% B. Six minutes after the injection, the proportion of A was linearly increased to 95% and for one additional minute to 98%. After this step, composition of the mobile phase was set to initial condition within 0.5 min and the column was equilibrated for 9.5 min prior to next injection. Retention times for the caged (**NPy-Ab**) and free pyranine (**Py-Ab**) were t_R = 5.9 min and t_R = 1.9 min respectively in these experimental conditions.

For **NPy-Ad**, the gradient used was as follow: Initially, the column was equilibrated with a mobile phase consisting of 70% A and 30% B. Six minutes after the injection, the proportion of A was linearly increased to 95% and for 1.5 additional minute to 98%. After this step, composition of the mobile phase was set to initial condition within 0.5 min and the column was equilibrated for 9.5 min prior to next injection. Retention times for the caged (**NPy-Ad**) and free pyranine (**Py-Ad**) were t_R = 8.7 min and t_R = 5.9 min respectively in these experimental conditions.

For **NPy-S**, the gradient used was as follow: Initially, the column was equilibrated with a mobile phase consisting of 50% C and 50% D. Four minutes after the injection, the proportion of C was linearly increased to 60%. After this step, composition of the mobile phase was set to initial condition within 0.5 min and the column was equilibrated for 5.5 min prior to next injection. Retention times for the

caged (**NPy-S**) and free pyranine (**HPTS**) were t_R = 3.9 min and t_R = 1.2 min respectively in these experimental conditions.

For **CPy-S**, the gradient used was as follow: Initially, the column was equilibrated with a mobile phase consisting of 10% A and 90% E. Two minutes after the injection, the proportion of A was linearly increased to 20% and for four additional minutes to 70%. After this step, composition of the mobile phase was set to initial condition within 0.5 min and the column was equilibrated for 5.5 min prior to next injection. Retention times for the caged (**CPy-S**) and free pyranine (**HPTS**) were t_R = 5.1 min and t_R = 1.6 min respectively in these experimental conditions.

Capillary electrophoresis (CE)

3 mL of a solution of the caged pyranine (**NPy-Ab**: 1 µM in 10 mM pH = 8.4 Trizma buffer) were placed in a quartz cuvette (1x1 cm^2) and submitted to irradiation at 365 nm LED under stirring. Aliquots of 30 µL were drawn at regular intervals and were subsequently analyzed by capillary electrophoresis. Capillary electrophoresis (CE) analysis was performed using a P/ACE MDQ capillary electrophoresis system equipped with LIF detector (with excitation at 488 nm and emission collection at 525 nm). The instrument was controlled and the data were collected and processed by the Beckman P/ACE 32 Karat software Version 8.0. Separations were performed in bare fused silica capillaries, (Polymicro, Phenix, AZ), 75 µm I.D. x 30 cm (20 cm to the detector). The running voltage was 20 kV. The temperature of the capillary cartridge was 25°C. Prior to separations, the capillary was rinsed with 0.1 M NaOH (40 psi for 1 min), water (20 psi, 1 min) and 20 mM CHES buffer pH 9.2 (20 psi, 1 min). Next, the sample was hydrodynamically injected for 5 s under 0.3 psi and a small plug of CHES buffer (0.2 psi for 2.0 sec) was introduced in the capillary before applying the separation voltage.

Theoretical derivation of the expression for retrieving light intensity

The model

We consider mechanisms of light-driven conversions, which can be reduced to the irreversible photochemical reaction displayed in Fig. S1.

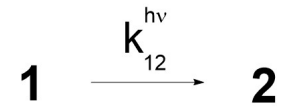

Fig. S1: Reduced mechanism accounting for the photoactivation of an actinometer **1** leading to the irreversible formation of the product **2**.

Since most such light-driven conversions involve multiple steps, this assumption implies that the light intensity is low enough to make the photochemical activation step rate-limiting.

We here consider that the irreversible photochemical reaction is performed in a closed system (overall volume V). Hence we write Eq.(S3) describing the evolution of the concentrations :

$$\frac{d1}{dt} = -\frac{d2}{dt} = -k_{12}\,1 \tag{S3}$$

where we can make explicit the photochemical contribution to the rate constant by writing

$$k_{12} = k_{12}^{h\nu}. \tag{S4}$$

We first derive the theoretical expressions of the concentrations in **1** and **2** (denoted 1 and 2 respectively) upon applying a light jump and establish the relation existing between the illumination time associated to the photochemical reaction and the photophysical and photochemical parameters associated to the photo-activation step. Then we analyze the time evolution of the absorbance and intrinsic/extrinsic fluorescence emission of the actinometer under illumination.

Expression of the concentrations

We consider that the system initially contains the actinometer **1** at concentration S_{tot}. The system is "suddenly"[a] illuminated, so that the incident photon flux varies from 0 to $\mathcal{I}$. The rate constant $k_{12} = k_{12}^{h\nu}$ can be considered constant. Upon writing $S_{\text{tot}} = 1 + 2$, Eq.(S3) yields:

$$1 = S_{\text{tot}} \exp\left(-\frac{t}{\tau}\right) \tag{S5}$$

$$2 = S_{\text{tot}}\left[1 - \exp\left(-\frac{t}{\tau}\right)\right] \tag{S6}$$

where

$$\tau = \frac{1}{k_{12}} \tag{S7}$$

[a] Note that "suddenly" here refers to a time interval such that Eq.(S3) can be considered valid.

designates the relaxation time (also often called characteristic time) associated to the photochemical reaction in the presence of light at constant photon flux $\mathcal{I}$. 5τ gives an estimate of the duration of the complete photoconversion of **1** into **2**.

The reaction rate for the photo-consumption of the actinometer **1** is proportional to the photon flux of the monochromatic excitation light absorbed by **1** at the excitation wavelength – written in both cases as, $\mathcal{I}_{\text{abs}}(\lambda_{\text{exc}})$, and to the unitless photo-consumption cross section, φ_{12}, which measures the probability of **1** photoactivation leading to **2** production after **1** light absorption:

$$-\frac{d1}{dt} = \frac{\mathcal{I}_{\text{abs}}(\lambda_{\text{exc}})\varphi_{12}}{V} \tag{S8}$$

where V is the irradiated volume (expressed in L or dm^3) and $\mathcal{I}_{\text{abs}}(\lambda_{\text{exc}})$ is expressed in E per unit of time.

$\mathcal{I}_{\text{abs}}(\lambda_{\text{exc}})$ is given by Eq.(S9)

$$\mathcal{I}_{\text{abs}}(\lambda_{\text{exc}}) \quad = \quad \frac{A_1(\lambda_{\text{exc}})}{A_{\text{tot}}(\lambda_{\text{exc}})}\mathcal{I}(\lambda_{\text{exc}}) \tag{S9}$$

where $A_1(\lambda_{\text{exc}})$ is the absorbance of **1**, $A_{\text{tot}}(\lambda_{\text{exc}})$ is the total absorbance, and $\mathcal{I}(\lambda_{\text{exc}})$ is the photon flux absorbed by the solution at the excitation wavelength. According to the Beer-Lambert law, the latter can be written

$$\mathcal{I}(\lambda_{\text{exc}}) \quad = \quad \mathcal{I}_0(\lambda_{\text{exc}})\left[1 - \exp\left(-2.3A_{\text{tot}}(\lambda_{\text{exc}})\right)\right] \tag{S10}$$

where $\mathcal{I}_0(\lambda_{\text{exc}})$ is the photon flux of the incident beam at the excitation wavelength.

We further consider that an actinometer is illuminated with a light source that perpendicularly illuminates a cuvette filled with its solution. Upon introducing the length of the optical pathlength ℓ and the molar absorption coefficient $\varepsilon_1(\lambda_{\text{exc}})$ (expressed in m^2.mol^{-1}) at the excitation wavelength,[b] Eq.(S8) yields

$$-\frac{d1}{dt} \quad = \quad \varepsilon_1(\lambda_{\text{exc}})\mathcal{I}_0(\lambda_{\text{exc}})\varphi_{12}\ell\frac{1 - exp\left(-2.3A_{\text{tot}}(\lambda_{\text{exc}})\right)}{A_{\text{tot}}(\lambda_{\text{exc}})V}1. \tag{S11}$$

If the total absorbance $A_{\text{tot}}(\lambda_{\text{exc}})$ is lower than 0.15, the kinetics is first order at first order with a rate constant k_{12} given in Eq.(S12)

$$k_{12} \quad = \quad 2.3\varepsilon_1(\lambda_{\text{exc}})\varphi_{12}\frac{\mathcal{I}_0(\lambda_{\text{exc}})\ell}{V} = 2.3\varepsilon_1(\lambda_{\text{exc}})\varphi_{12}I_0(\lambda_{\text{exc}}) \tag{S12}$$

upon introducing the incident light intensity $I_0(\lambda_{\text{exc}})$ (expressed in E.m^{-2}.s^{-1}).

Eq. (S12) can be alternatively written by introducing the cross section for the photochemical reaction $\sigma_{12}(\lambda_{\text{exc}})$

$$\sigma_{12}(\lambda_{\text{exc}}) = 2.3\varepsilon_1(\lambda_{\text{exc}})\varphi_{12} \tag{S13}$$

which yields

$$k_{12} = \frac{1}{\tau} = \sigma_{12}(\lambda_{\text{exc}})I_0(\lambda_{\text{exc}}). \tag{S14}$$

[b] Note that the unit of $\varepsilon(\lambda)$ is in m^2.mol^{-1}. One has: $\varepsilon(\lambda)$(m^2.mol^{-1})=0.1$\times\varepsilon(\lambda)$(mol.L^{-1}.cm^{-1}).

Eq.(S12) shows that the rate constant k_{12} can be evaluated from the knowledge of the photophysical and photochemical parameters, $\varepsilon_1(\lambda_{exc})$ and φ_{12} or $\sigma_{12}(\lambda_{exc})$, as soon as $I_0(\lambda_{exc})$ is known. Conversely, $I_0(\lambda_{exc})$ can be retrieved from Eq.(S15) from the knowledge of $\varepsilon_1(\lambda_{exc})$ and φ_{12} or $\sigma_{12}(\lambda_{exc})$, and the relaxation time of the photochemical reaction τ.

$$I_0(\lambda_{exc}) = \frac{k_{12}}{2.3\varepsilon_1(\lambda_{exc})\varphi_{12}} = \frac{1}{2.3\varepsilon_1(\lambda_{exc})\varphi_{12}\tau} = \frac{1}{\sigma_{12}(\lambda_{exc})\tau} \quad \text{(S15)}$$

In order to simplify the notations, we identified $I_0(\lambda_{exc})$ to $I(\lambda_{exc})$ and $\sigma_{12}(\lambda_{exc})$ to $\sigma(\lambda_{exc})$ in the Main Text.

Photoactivation of a caged fluorophore in confocal microscopy

The kinetic behavior of a caged fluorophore observed in confocal microscopy differs from the one observed in the cuvette experiments or in epifluorescence microscopy since illumination is not continuous but transient. Upon the short exposure to illumination during the dwell time-long scan at a pixel (microsecond range), the dark caged pyranine derivative is photoactivated and engaged in the thermal steps of the uncaging mechanism. However it has most probably not enough time to liberate the corresponding bright fluorophore. In contrast, at the time scale of the image scanning (second range), the whole set of thermal steps of the uncaging mechanism has enough time to take place. Hence, at the later time scale, the time evolution of the fluorescence signal can be reliably accounted for with a two-state kinetic model in which the dark caged pyranine derivative yields the corresponding bright fluorophore in one photochemical step, which is associated with the rate constant σI where σ designates the cross section associated with the photoactivation.

We are interested in the overall fluorescence signal arising from scanning a solution of caged pyranine derivative sandwiched between two glass slides with the focused laser of the microscope. We respectively denote $R(x,y,z,t)$ and $P(x,y,z,t)$ the concentrations of caged pyranine (subsequently denoted **R**) and liberated fluorophore (subsequently denoted **P**) at position (x,y,z) and time t.

We first model the illumination profile in time and space. The sample is exposed to illumination of moving light intensity $I\left(x'\left(t\right),y'\left(t\right),z'\left(t\right)\right)$ of the laser beam. In confocal microscopy, illumination is not homogeneous over the field of view and fluorescence collection is spatially limited (e.g. by using a pinhole). It is often considered that illumination leading to fluorescence collection results from a focused laser beam assumed to adopt a radially and axially Gaussian intensity profile given in Eq.(S16)

$$I_{\text{Gaussian}}\left(x',y',z'\right) \quad = \quad I_0 \exp\left[-2\left(\frac{x'^2+y'^2}{w_0^2}\right)\right]\exp\left[-2\left(\frac{z'^2}{z_0^2}\right)\right] \quad \text{(S16)}$$

where I_0, w_0, and z_0 designate the light intensity at coordinates $(0,0,0)$, the waist radius in the focal plane, and the radial resolution z_0 respectively (see Fig. S2).[c]

In order to facilitate the following calculations, we assimilated the Gaussian illumination given in Eq.(S16) to uniform illumination in the square cuboid given in Eqs. (S17,S18)

$$I_{\text{Cuboid}}\left(x',y',z'\right) \quad = \quad I \quad \text{(S17)}$$

[c] As a consequence, Eq. S16 is valid only for lenses of relatively low NA (which have a cylindrical illumination profile).

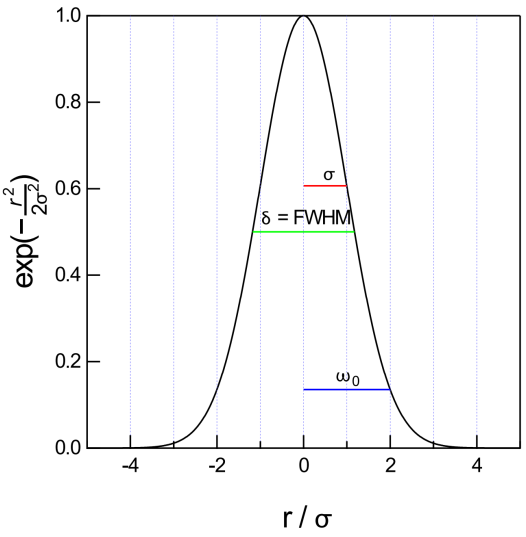

Fig. S2: *Cross-section of the Gaussian beam for* z' = z_0. $\omega_0 = 2\sigma$ and I_0 corresponds to the maximum.

for $-\frac{\omega_0}{2} \leq x' \leq \frac{\omega_0}{2}$, $-\frac{\omega_0}{2} \leq y' \leq \frac{\omega_0}{2}$, and $-\frac{z_0}{2} \leq z' \leq \frac{z_0}{2}$, and

$$I_{\text{Cuboid}}\left(x', y', z'\right) \quad = \quad 0 \tag{S18}$$

in the remaining space. Upon constraining the integrals over the volume of the illumination profile to be the same with both geometrical models

$$\int_{-\infty}^{\infty}\int_{-\infty}^{\infty}\int_{-\infty}^{\infty} I_{\text{Gaussian}} dxdydz \quad = \quad \int_{-\infty}^{\infty}\int_{-\infty}^{\infty}\int_{-\infty}^{\infty} I_{\text{Cuboid}} dxdydz \tag{S19}$$

one has then

$$I \quad = \quad \left(\sqrt{\frac{\pi}{2}}\right)^{\frac{3}{2}} I_0 \simeq 2I_0 \tag{S20}$$

Then we considered the laser beam of the confocal microscope to scan the sample along a single line parallel to the x-axis with a constant scanning speed v. Due to scanning, the x'-coordinate of the maximum I of the light intensity profile is a function of time: $I\left(x'\left(t\right), y', z'\right)$. We consider scanning to start at $x' = -\ell/2$ and end up at $x' = \ell/2$ with $x'\left(t\right) = vt - \ell/2$ and T to be the time it takes for the scanning beam to cross the line with length ℓ at constant scanning speed $v = \ell/T$. Using the two-state kinetic model in which the dark caged pyranine derivative yields the corresponding bright fluorophore, the time evolution of the concentrations of **R** and **P** at position (x, y, z) is accounted by Eq.(S21)

$$\frac{\partial R\left(x, y, z, t\right)}{\partial t} \quad = \quad -\sigma I\left(x'\left(t\right), y'\left(t\right), z'\left(t\right)\right) R\left(x, y, z, t\right) \tag{S21}$$

We denote $R_0\left(x, y, z\right)$ the initial concentration of the **R** state at the coordinate (x, y, z) before starting to record the first line (the concentration of the **P** state is initially zero). Then the concentrations of **R** and **P** evolve in time as follows:

- $0 \leq t \leq t_{\text{min}} = (x + \ell/2 - \omega_0/2)/v$

$$R(x,y,z,t) = R_0(x,y,z) \quad \text{(S22)}$$

$$P(x,y,z,t) = 0 \quad \text{(S23)}$$

- $t_{\text{min}} = (x + \ell/2 - \omega_0/2)/v \leq t \leq t_{\text{max}} = (x + \ell/2 + \omega_0/2)/v$

$$R(x,y,z,t) = R_0(x,y,z)\, e^{-\sigma I(t-t_{\text{min}})} \quad \text{(S24)}$$

$$P(x,y,z,t) = R_0(x,y,z)\left[1 - e^{-\sigma I(t-t_{\text{min}})}\right] \quad \text{(S25)}$$

- $t_{\text{max}} = (x + \ell/2 + \omega_0/2)/v$

$$R(x,y,z,t) = R_0(x,y,z)\, e^{-\sigma I(t_{\text{max}}-t_{\text{min}})} = R_0(x,y,z)\, e^{-\sigma I\frac{\omega_0}{v}} \quad \text{(S26)}$$

$$P(x,y,z,t) = R_0(x,y,z)\left[1 - e^{-\sigma I(t_{\text{max}}-t_{\text{min}})}\right] = R_0(x,y,z)\left[1 - e^{-\sigma I\frac{\omega_0}{v}}\right] \quad \text{(S27)}$$

Beyond t_{max}, the thermal relaxation of the **R** photoactivated state becomes active but the signal recorded at each pixel is the one measured at t_{max}. Introducing the brightness Q_R and Q_P of **R** and **P** respectively, the fluorescence signal $F(x,y,z)$ at position (x,y,z) after time T results from the scanning occurring between the times t_{min} and t_{max}. It is given in Eq.(S28)

$$F(x,y,z,T) = \int_{t_{\text{min}}}^{t_{\text{max}}} I \times \left\{ Q_R R_0(x,y,z)\, e^{-\sigma I(t-t_{\text{min}})} + Q_P R_0(x,y,z)\left[1 - e^{-\sigma I(t_{\text{max}}-t_{\text{min}})}\right]\right\} dt \quad \text{(S28)}$$

$$= Q_P R_0(x,y,z)\, I\frac{\omega_0}{v} + (Q_R - Q_P)\, R_0(x,y,z)\,\frac{1}{\sigma}\left[1 - e^{-\sigma I\frac{\omega_0}{v}}\right] \quad \text{(S29)}$$

Finally, the overall fluorescence signal gathered from scanning the whole volume V with the illumination profile after time T is

$$F_V(T) = \int_{-\ell/2}^{\ell/2}\int_{-\omega_0/2}^{\omega_0/2}\int_{-z_0/2}^{z_0/2} F(x,y,z,T)\, dxdydz \quad \text{(S30)}$$

$$= Q_P\langle R_0(x,y,z)\rangle_V V I\frac{\omega_0}{v} + (Q_R - Q_P)\,\langle R_0(x,y,z)\rangle_V V\frac{1}{\sigma}\left[1 - e^{-\sigma I\frac{\omega_0}{v}}\right] \quad \text{(S31)}$$

where $\langle R_0(x,y,z)\rangle_V$ designates the average initial concentration of the **R** state over the volume V.

In practice, we acquired a set of square frames, which have been scanned by the laser focus along both the x and y axes. In the scanning process, the square is built by sequentially scanning lines distant from the pixel size Δy. When the beam waist ω_0 is larger than the pixel size Δy, the caged pyranine derivatives are exposed more than one time to the light during acquisition of an image frame. More precisely, they are exposed $\omega_0/\Delta y$ times to the light intensity. Hence, after the collection of the first image frame F_1, the concentrations of **R** and **P** are

$$R(x,y,z,t) = R_0(x,y,z)\, e^{-\sigma I\frac{\omega_0^2}{v\Delta y}} \quad \text{(S32)}$$

$$P(x,y,z,t) = R_0(x,y,z)\left[1 - e^{-\sigma I\frac{\omega_0^2}{v\Delta y}}\right] \quad \text{(S33)}$$

and the overall fluorescence signal gathered from scanning the whole volume V with the illumination profile is

$$F_V\left(F_1\right) = Q_P\langle R_0\left(x,y,z\right)\rangle_V V I\frac{\omega_0^2}{v\Delta y} + \left(Q_R - Q_P\right)\langle R_0\left(x,y,z\right)\rangle_V V\frac{1}{\sigma}\left[1 - e^{-\sigma I\frac{\omega_0^2}{v\Delta y}}\right] \quad \text{(S34)}$$

More generally, after the collection of the n-th image frame F_n, the concentrations of **R** and **P** are

$$R\left(x,y,z,t\right) = R_0\left(x,y,z\right)e^{-n\sigma I\frac{\omega_0^2}{v\Delta y}} \quad \text{(S35)}$$

$$P\left(x,y,z,t\right) = R_0\left(x,y,z\right)\left[1 - e^{-n\sigma I\frac{\omega_0^2}{v\Delta y}}\right] \quad \text{(S36)}$$

and the overall fluorescence signal gathered from scanning the whole volume V with the illumination profile is

$$F_V\left(F_n\right) = Q_P\langle R_0\left(x,y,z\right)\rangle_V V I\frac{\omega_0^2}{v\Delta y} + \left(Q_R - Q_P\right)\langle R_0\left(x,y,z\right)\rangle_V V\frac{1}{\sigma}\left[1 - e^{-n\sigma I\frac{\omega_0^2}{v\Delta y}}\right] \quad \text{(S37)}$$

Upon introducing the dwell time $\delta = \Delta y/v$, Eq.(S37) yields Eq.(S38)

$$F_V\left(F_n\right) = Q_P\langle R_0\left(x,y,z\right)\rangle_V V I\frac{\omega_0^2}{\Delta y^2}\delta + \left(Q_R - Q_P\right)\langle R_0\left(x,y,z\right)\rangle_V V\frac{1}{\sigma}\left[1 - e^{-n\delta\sigma I\frac{\omega_0^2}{\Delta y^2}}\right]. \quad \text{(S38)}$$

Eq.(S37) shows that the light intensity I can be retrieved from investigating the monoexponential dependence of the overall fluorescence signal $F_V\left(F_n\right)$ on the number of frame n or similarly on the light exposure time $t = n\delta$. Indeed, the extracted characteristic time $\tau = \frac{1}{\sigma I}\frac{\Delta y^2}{\omega_0^2}$ yields I once σ, Δy, and ω_0 are known.

In order to extract the value of the uncaging cross section of the caged pyranines σ retrieved in the Main Text from the observed rise of fluorescence intensity as a function of $t = n\tau$, we further had to measure:

- The pixel size Δy, which is fixed for recording an image in confocal microscopy;
- The value of w_0, which we measured with Raster image correlation spectroscopy;[5,6]
- The light intensity I with a powermeter. A powermeter spatially integrates light intensity over all its detecting element and delivers $\frac{1}{2}I_0\pi w_0^2$ (obtained by 2D integration of the Gaussian beam). With our confocal microscope, scanning is performed at constant speed along the x-axis and light application effectively occurs only during a fraction γ of the period of the sinusoidal motion of the focal point.[d] Hence, the power experienced by the sensor during scanning is $P = \frac{\gamma}{2}I_0\pi w_0^2$. Equipped with the values of w_0 and the γ parameter, it subsequently becomes possible to retrieve the $I = 2I_0 = \frac{4}{\gamma\pi w_0^2}P$ value from the light power measured with the powermeter.

[d] To evaluate the fraction γ, the sensitive element of a fast photodiode (PD10A, Thorlabs, NJ) was placed at the focal plane of the imaging objective during acquisition of a series of 30 images. The output signal from the photodiode was digitized by a 300 MHz oscilloscope (RTB2004, Rhode and Schwarz, Munich, Germany) and we measured $\gamma = 0.4$, indicating that the laser excitation is turned off when the beam returns to the initial x position between line scans to reduce photo-damage to the sample.

Supplementary Figures

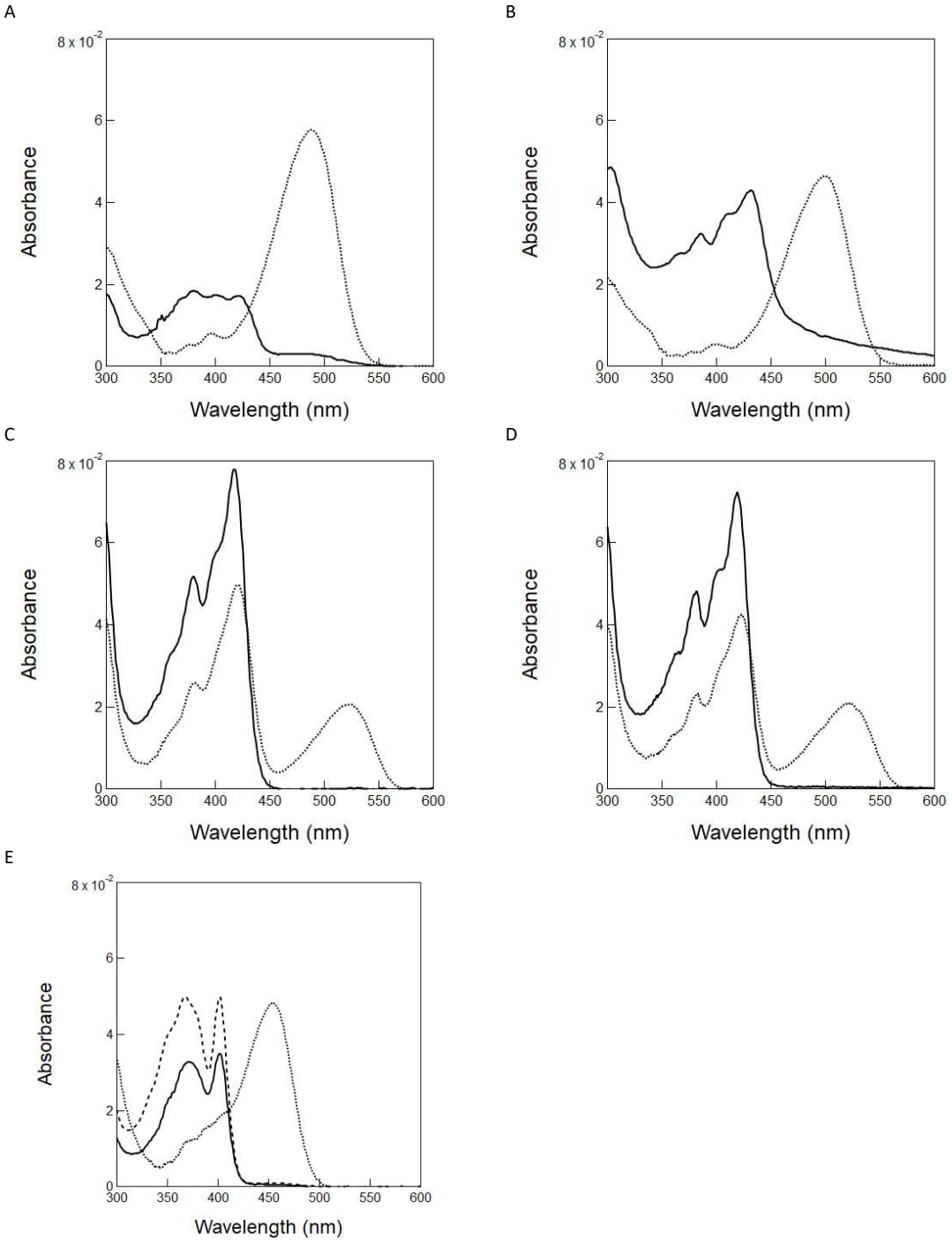

Fig. S3 *UV-Vis absorption spectra of the free and caged pyranine derivatives*. Absorption spectra of the free (dotted lines) and caged (solid lines) pyranine derivatives **Py-Aa** and **NPy-Aa** (A), **Py-Ab** and **NPy-Ab** (B), **Py-Ac** and **NPy-Ac** (C), **Py-Ad** and **NPy-Ad** (D), and **HPTS**, **NPy-S** and **CPy-S** (E; solid line: **NPy-S**; dashed line: **CPy-S**). The spectra were recorded at 2 µM concentration in 10 mM pH 7.4 PBS (for **Py-Aa-b** and **NPy-Aa-b**), 1 mM pH = 8.4 Trizma buffer/acetonitrile 1/19 (v/v) (for **Py-Ac-d** and **NPy-Ac-d**), and 10 mM pH = 8.4 Trizma buffer (for **HPTS**, **NPy-S** and **CPy-S**). *T* = 293 K.

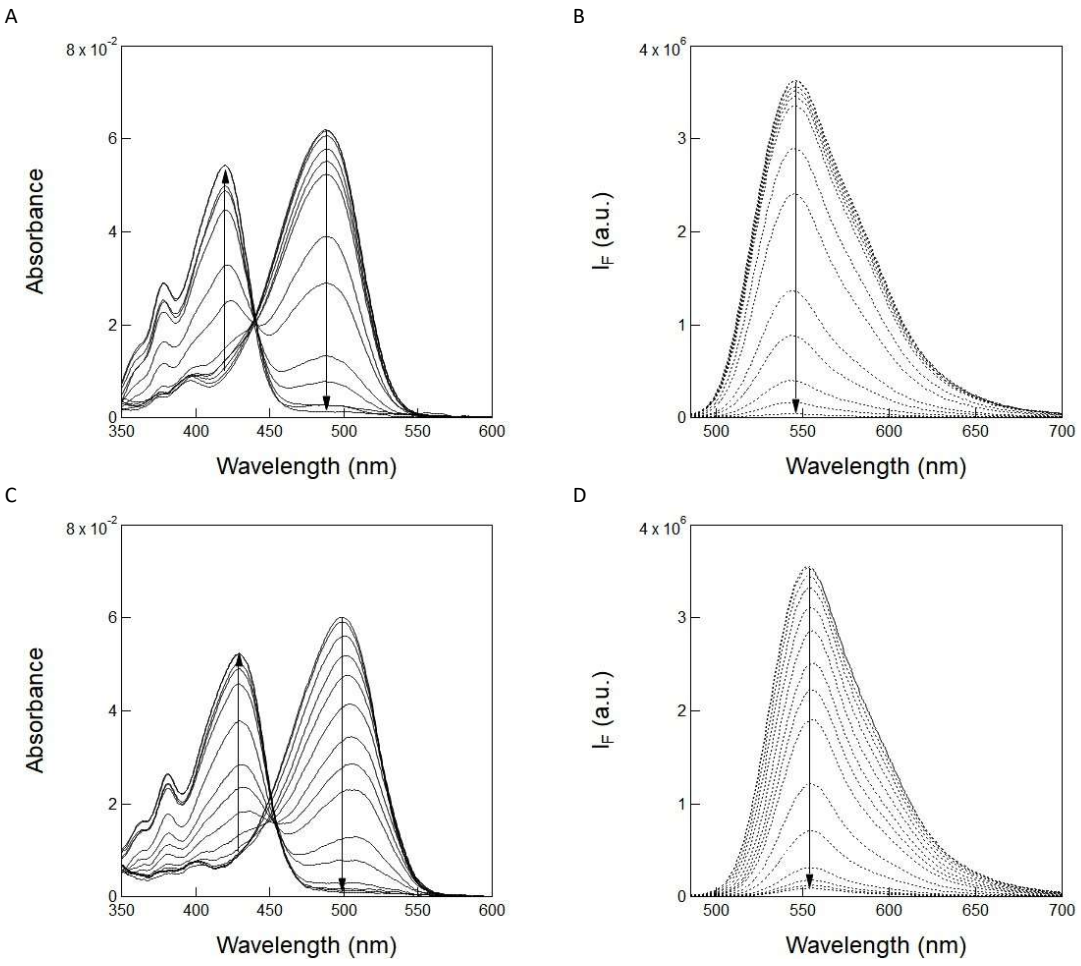

Fig. S4 *Determination of the proton exchange constants of the free pyranine derivatives **Py-Aa** and **Py-Ab***. pH-dependence of the absorption (solid lines) and emission (dotted lines; λ_{exc} = 480 nm) spectra of **Py-Aa** (A and B) and **Py-Ab** (C and D) recorded at 2 μM in 10 mM universal buffer. pH = 9.02, 8.46, 7.47, 7.11, 6.90, 6.71, 6.25, 5.85, 5.32, 5.00, 4.55, 4.05, 2.90 for **Py-Aa** and pH = 9.01, 8.44, 7.47, 6.83, 6.50, 5.97, 5.47, 5.11, 4.86, 4.40, 3.98, 3.47, 3.04, 2.69, 2.41 for **Py-Ab.** *T* = 293 K.

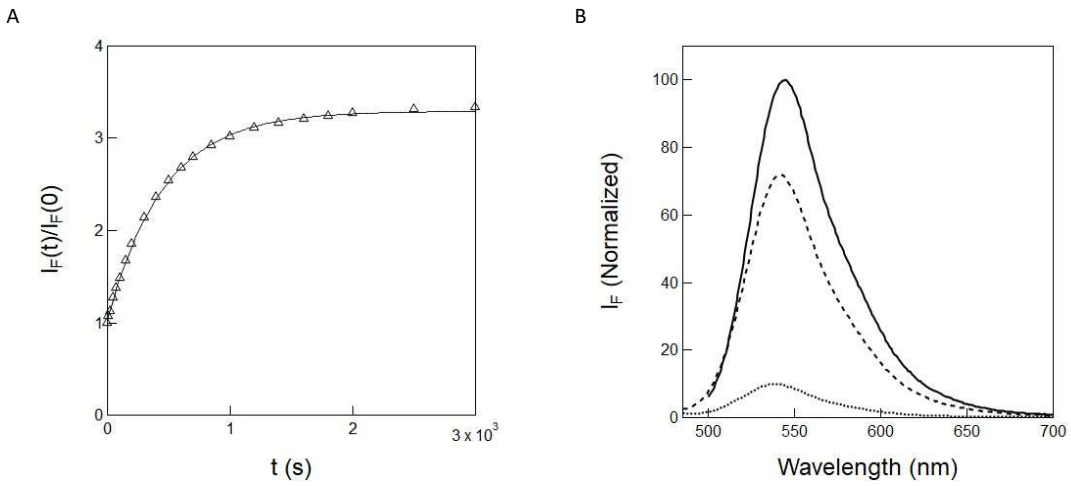

Fig. S5 A: *Preliminary evidence for uncaging in **NPy-Aa***. Temporal evolution of the fluorescence emission at λ_{em}= 540 nm upon homogeneous illumination of 2 μM **NPy-Aa** in 10 mM pH 7.4 PBS contained in a 54 μL cuvette (3 mm optical pathlength) with the LED at λ_{exc}=(365±25) nm (2.5×10^{-8} E.s^{-1}; 1.4×10^{-3} E.m^{-2}.s^{-1}). Markers: experimental data, solid line: monoexponential fit to Eq. (S1); the characteristic time τ = 460 s has been retrieved from A at *T* = 293 K; B: Preliminary evaluation of the uncaging yield in **NPy-Aa**. Comparison of the fluorescence emission spectra recorded at a same 2 μM concentration in 10 mM pH 7.4 PBS from the free pyranine derivative **Py-Aa** (solid line), the caged pyranine derivative **NPy-Aa** (dotted line), and the caged pyranine derivative **NPy-Aa** after illuminating with the LED at λ_{exc}=(365±25) nm (2.5×10^{-8} E.s^{-1}; 1.4×10^{-3} E.m^{-2}.s^{-1}) up to the stabilization of the fluorescence signal (dashed line recorded after time t = 3500 s). *T* = 293 K.

Fig. S5 reports on the behavior of the caged pyranine ***NPy-Aa*** in 10 mM pH 7.4 PBS under illumination at 365 nm at 2.5×10^{-8} E.s^{-1} light intensity and 1.4×10^{-3} E.m^{-2}.s^{-1} photon flux density. We observed an increase of its fluorescence by a factor 3 and computed an uncaging yield of 62% from comparing the final signal with the one of the free pyranine ***Py-Aa*** at the same concentration in the same solvent. Moreover, from fitting the time fluorescence emission with a monoexponential function, we retrieved 1.6±0.2 m^2.mol^{-1} for the associated cross section σ. The caged pyranine ***NPy-Aa*** has not been further investigated since it revealed unable to cross the cell bilayers, which had been an initial requested specification for its development.

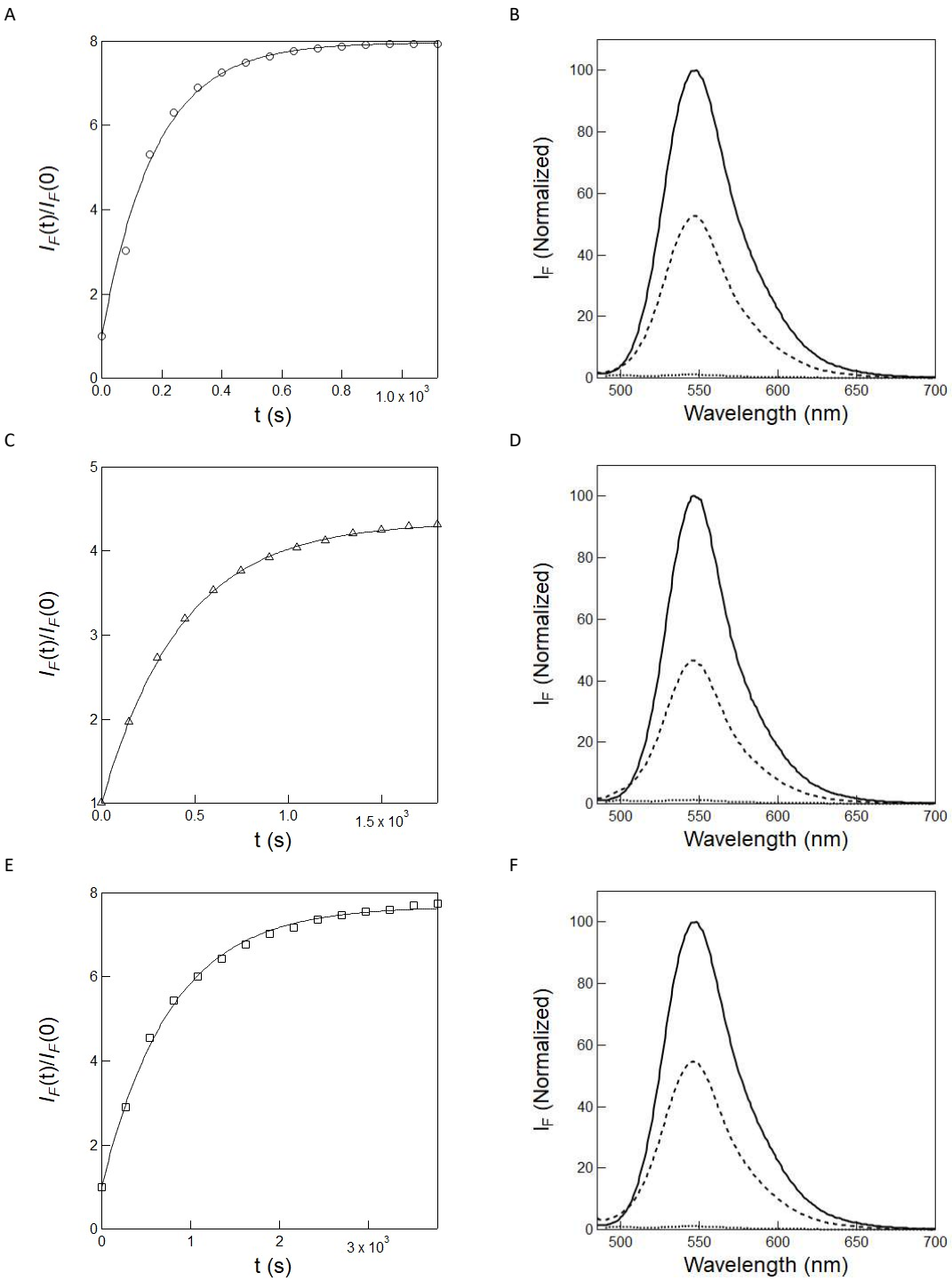

Fig. S6 A,C,E: *Preliminary evidence for uncaging in **NPy-Ab***. Temporal evolution of the fluorescence emission at λ_{em}= 540 nm upon homogeneous illumination of 1 µM **NPy-Ab** in 10 mM pH 8.4 Trizma buffer contained in a 54 µL cuvette (3 mm optical pathlength) with the LED at λ_{exc}=(365±25) nm (A: 1.6×10^{-8} E.s^{-1}, 8.7×10^{-4} E.m^{-2}.s^{-1}; C: 7.2×10^{-9} E.s^{-1}, 4.0×10^{-4} E.m^{-2}.s^{-1}; E: 2.9×10^{-9} E.s^{-1}, 1.6×10^{-4} E.m^{-2}.s^{-1}). Markers: experimental data, solid line: exponential fit to Eq. (S1); the characteristic times τ = 177 s, τ = 425 s, and τ = 771 s have been retrieved from A, C and E respectively at *T* = 293 K; B,D,F: Preliminary evaluation of the uncaging yield in **NPy-Ab**. Comparison of the fluorescence emission spectra recorded at a same 2 µM concentration in 10 mM pH 8.4 Trizma buffer from the free pyranine derivative **Py-Ab** (solid line), the caged pyranine derivative **NPy-Ab** (dotted line), and the caged pyranine derivative **NPy-Ab** after illuminating with the LED at λ_{exc}=(365±25) nm (B: 2.5×10^{-8} E.s^{-1}, 1.4×10^{-3} E.m^{-2}.s^{-1}; D: 1.1×10^{-8} E.s^{-1}, 6.2×10^{-4} E.m^{-2}.s^{-1}; F: 5.1×10^{-9} E.s^{-1}, 2.8×10^{-4} E.m^{-2}.s^{-1}) up to the stabilization of the fluorescence signal (dashed line recorded after time t; B: t = 1000 s; D: t = 1800 s; F: t = 3600 s). *T* = 293 K.

Fig. S6 displays the impact of light intensity on **NPy-Ab** uncaging in 10 mM pH 8.4 Trizma buffer at light intensities ranging from 0.3 to 1.6 10^{-8} E.s^{-1} ((1.6-8.7) 10^{-4} E.m^{-2}.s^{-1}). The drop of light intensity does not govern any significant modification of both the contrast between the final and initial fluorescence signal (around 6) and the uncaging yield (around 45%). The characteristic time retrieved from applying a monoexponential fit is essentially inversely proportional to the light intensity and leads to a photoactivation cross section σ equal to 6.8±0.7 m^2.mol^{-1}.

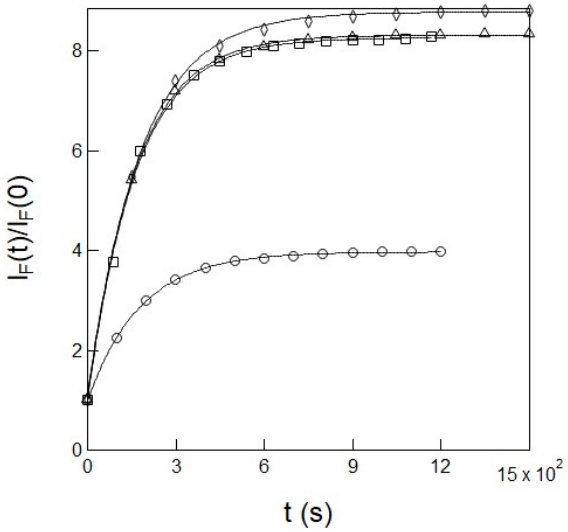

Fig. S7 *Significance of concentration on **NPy-Ab** uncaging at 365 nm*. Time evolution of the normalized fluorescence emission at 550 nm from 0.1 (circles), 0.5 (squares), 1 (triangles), and 2 µM (diamonds) **NPy-Ab** in 10 mM pH = 8.4 Trizma buffer in a 54 µL cuvette (3 mm optical pathlength) upon irradiation at constant light intensity of 15.6×10^{-9} E.s^{-1} at 365 nm. Markers: Experimental data; solid lines: Monoexponential fit with Eq. (S1); the characteristic times (s): 180, 164, 162 and 177 have been retrieved at the different concentration of **NPy-Ab**. *T* = 293 K.

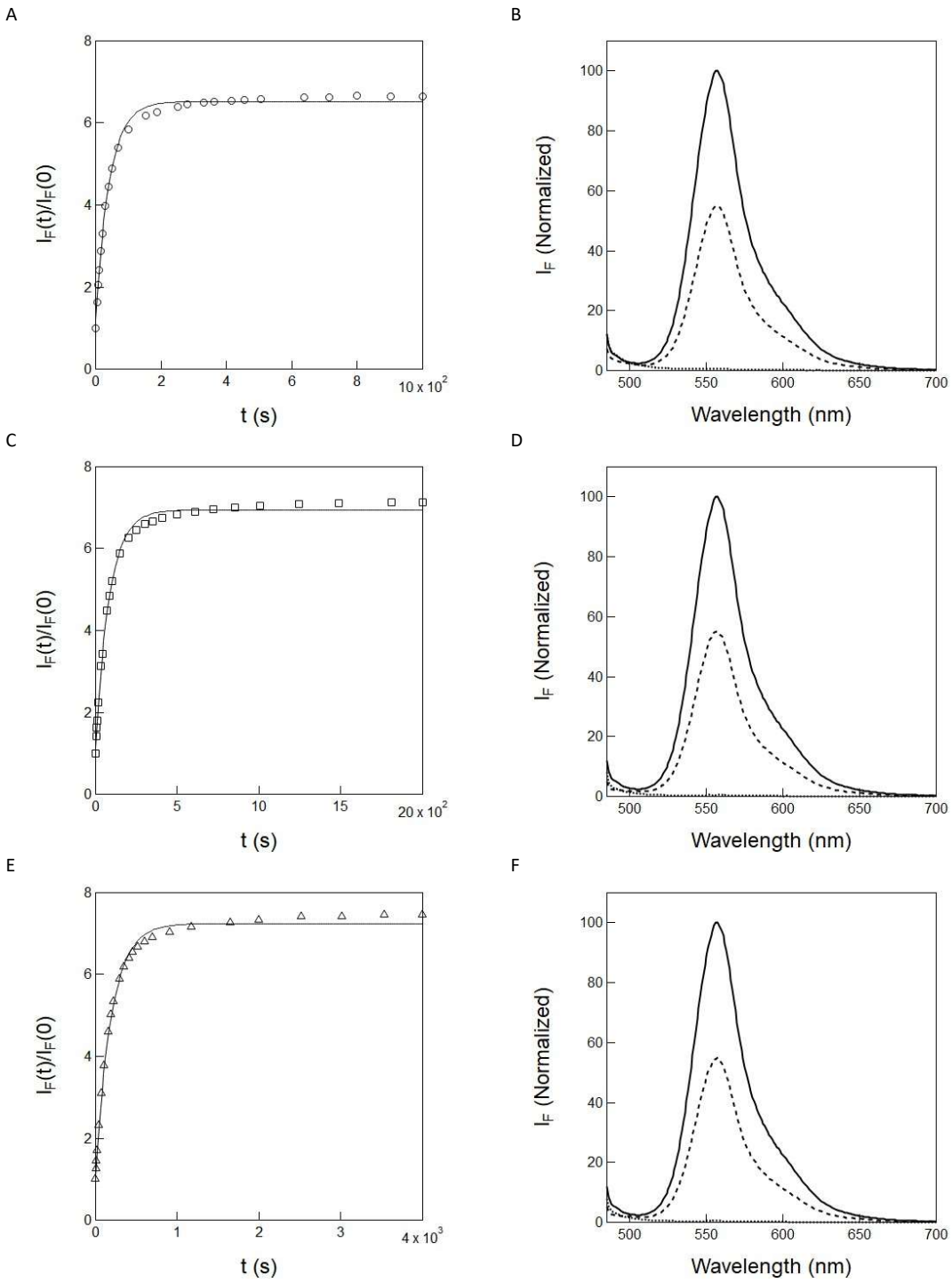

Fig. S8 A,C,E: *Preliminary evidence for uncaging in **NPy-Ac***. Temporal evolution of the fluorescence emission at λ_{em}= 540 nm upon homogeneous illumination of 2 μM ***NPy-Ac*** in 1 mM pH = 7.4 PBS/acetonitrile 1/19 (v/v) contained in a 54 μL cuvette (3 mm optical pathlength) with the LED at λ_{exc}=(365±25) nm (A: 2.5×10^{-8} E.s^{-1}, 1.4×10^{-3} E.m^{-2}.s^{-1}; C: 1.1×10^{-8} E.s^{-1}, 6.2×10^{-4} E.m^{-2}.s^{-1}; E: 5.1×10^{-9} E.s^{-1}, 2.8×10^{-4} E.m^{-2}.s^{-1}). Markers: experimental data, solid line: monoexponential fit to Eq. (S1); the characteristic time τ = 42 s, τ = 84 s and τ = 193 s have been retrieved from A, C, and E respectively at *T* = 293 K; B,D,F: *Preliminary evaluation of the uncaging yield in**NPy-Ac***. Comparison of the fluorescence emission spectra recorded at a same 2 μM concentration in 1 mM pH = 7.4 PBS/acetonitrile 1/19 (v/v) from the free pyranine derivative ***Py-Ac*** (solid line), the caged pyranine derivative ***NPy-Ac*** (dotted line), and the caged pyranine derivative ***NPy-Ac*** after illuminating with the LED at λ_{exc}=(365±25) nm (B: 2.5×10^{-8} E.s^{-1}, 1.4×10^{-3} E.m^{-2}.s^{-1}; D: 1.1×10^{-8} E.s^{-1}, 6.2×10^{-4} E.m^{-2}.s^{-1}; F: 5.1×10^{-9} E.s^{-1}, 2.8×10^{-4} E.m^{-2}.s^{-1}) up to the stabilization of the fluorescence signal (dashed line recorded after time *t*; B: *t* = 1000 s; D: *t* = 2000 s; F: *t* = 4000 s). *T* = 293 K.

Fig. S8 displays the impact of light intensity on **NPy-Ac** uncaging at light intensities ranging from 0.5 to 2.5 10^{-8} E.s^{-1} ((2.8-14) 10^{-4} E.m^{-2}.s^{-1}) in pH = 7.4 PBS buffer: acetonitrile 1:19 (v:v). In the examined range of timescales (0-4 10^3 s), we applied a monoexponential fitting function and retrieved a characteristic time essentially inversely proportional to the light intensity, which yielded 18.3±2.0 m^2.mol^{-1} for the associated cross section σ for **NPy-Ac**. The latter cross section is in fair agreement with the corresponding value extracted for **NPy-Ad** as anticipated from the similar sulfonamide functions in both **NPy-Ac** and **NPy-Ad**. Yet, we noticed a departure from the monoexponential behavior at the longest times, which has suggested a second slow process to take place. Since the dimethylamino substituents in **NPy-Ac** are less bulky than the piperidine ones in **NPy-Ad**, we envision that deaggregation would be less favored in **NPy-Ac** than in **NPy-Ad**. Hence, we preferred to retain **NPy-Ad** instead of **NPy-Ac** for measuring light intensity in hydrophobic media in order to make data processing at the most robust.

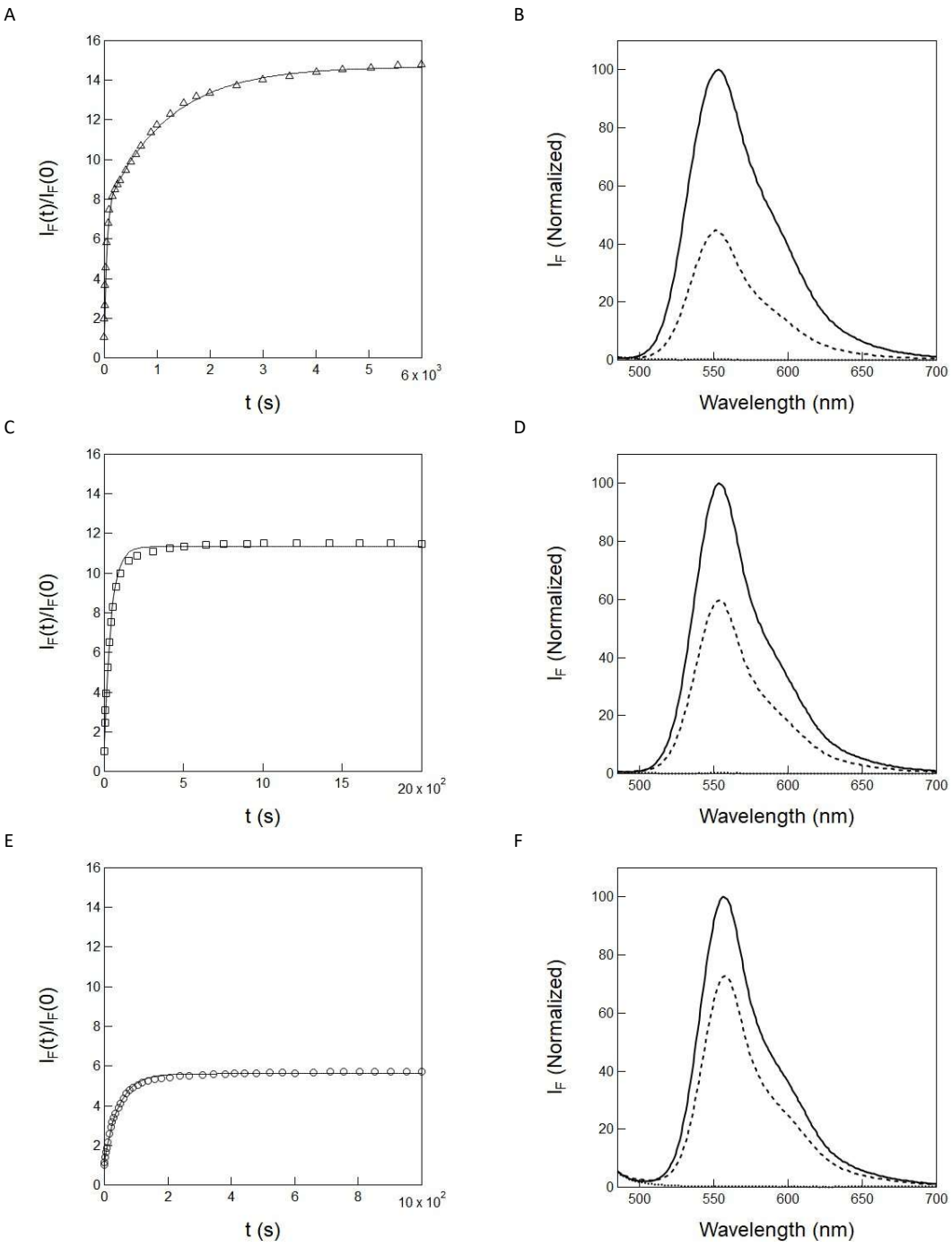

Fig. S9 A,C,E: *Preliminary evidence for uncaging in **NPy-Ad***. Temporal evolution of the fluorescence emission at λ_{em}= 540 nm upon homogeneous illumination of 2 μM **NPy-Ad** in (A: 10 mM pH = 7.4 PBS/acetonitrile 1/1 (v/v); C: 2 mM pH = 7.4 PBS/acetonitrile 1/4 (v/v); E: 1 mM pH = 7.4 PBS/acetonitrile 1/19 (v/v)) contained in a 54 μL cuvette (3 mm optical pathlength) with the LED at λ_{exc}=(365±25) nm at 2.5×10^{-8} E.s^{-1}, 1.4×10^{-3} E.m^{-2}.s^{-1}. Markers: experimental data, solid line: biexponential fit to Eq. (S2) (A) and monoexponential fit to Eq. (S1) (C,E); the characteristic times τ_1 = 44 s and τ_2 = 1170 s, τ = 44 s, and τ = 46 s have been retrieved from A, C, and E respectively at *T* = 293 K; B,D,F: Preliminary evaluation of the uncaging yield in **NPy-Ad**. Comparison of the fluorescence emission spectra recorded at a same 2 μM concentration in (B: 10 mM pH = 7.4 PBS/acetonitrile 1/1 (v/v); D: 2 mM pH = 7.4 PBS/acetonitrile 1/4 (v/v); F: 1 mM pH = 7.4 PBS/acetonitrile 1/19 (v/v)) from the free pyranine derivative **Py-Ad** (solid line), the caged pyranine derivative **NPy-Ad** (dotted line), and the caged pyranine derivative **NPy-Ad** after illuminating with the LED at λ_{exc}=(365±25) nm at 2.5×10^{-8} E.s^{-1}, 1.4×10^{-3} E.m^{-2}.s^{-1} up to the stabilization of the fluorescence signal (dashed line recorded after time t; B: t = 6000 s; D: t = 2000 s; F: t = 1000 s). *T* = 293 K.

Fig. S9 displays the impact of the solvent as a mixture of acetonitrile and aqueous pH = 7.4 PBS buffer on **NPy-Ad** uncaging. Shifting the ratio of acetonitrile to buffer from 1:1 to 19:1 (v:v) governs: (i) a change from a biexponential to a monoexponential time evolution of the fluorescence signal. The shortest retrieved characteristic time is found essentially constant equal to 44 s at 2.5×10^{-8} $E.s^{-1}$ light intensity and 1.4×10^{-3} $E.m^{-2}.s^{-1}$ photon flux density; (ii) a decay of the contrast between the final and initial fluorescence signal from 15 to 6; (iii) an increase of the uncaging yield from 45 to 72%.

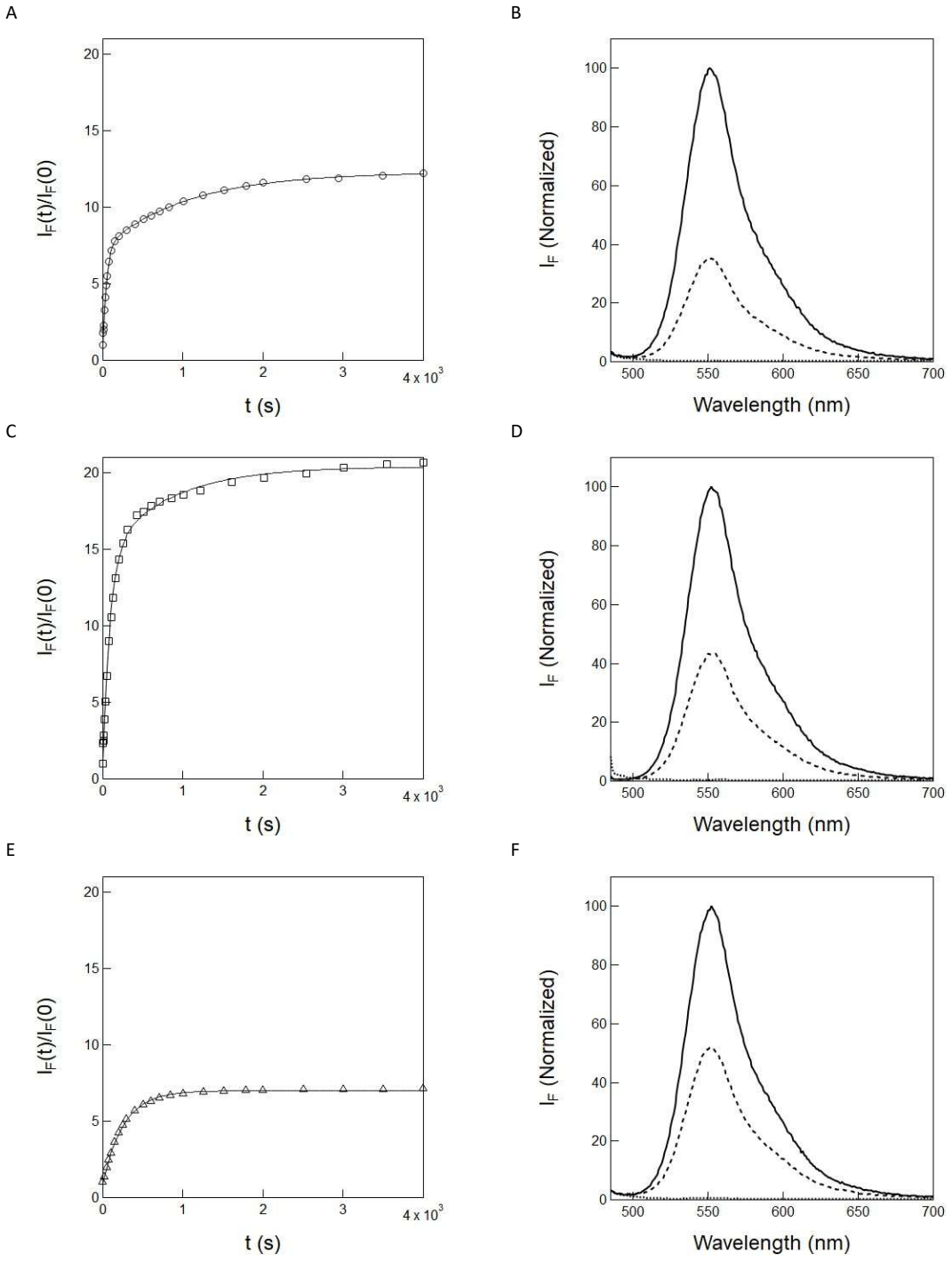

Fig. S10 A,C,E: *Preliminary evidence for uncaging in **NPy-Ad***. Temporal evolution of the fluorescence emission at λ_{em}= 540 nm upon homogeneous illumination of 0.2 μM **NPy-Ad** in 10 mM pH = 7.4 PBS/acetonitrile 1/1 (v/v) contained in a 54 μL cuvette (3 mm optical pathlength) with the LED at λ_{exc}=(365±25) nm (A: 2.5×10^{-8} E.s^{-1}, 1.4×10^{-3} E.m^{-2}.s^{-1}; C: 1.1×10^{-8} E.s^{-1}, 6.2×10^{-4} E.m^{-2}.s^{-1}; E: 5.1×10^{-9} E.s^{-1}, 2.8×10^{-4} E.m^{-2}.s^{-1}). Markers: experimental data, solid line: biexponential fit to Eq. (S2) (A,C) and monoexponential fit to Eq. (S1) (E); the characteristic times τ_1 = 46 s and τ_2 = 1061 s, τ_1 = 92 s and τ_2 = 814 s, and τ = 262 s have been retrieved from A, C, and E respectively at *T* = 293 K; B,D,F: Preliminary evaluation of the uncaging yield in **NPy-Ad**. Comparison of the fluorescence emission spectra recorded at a same 2 μM concentration in 10 mM pH = 7.4 PBS/acetonitrile 1/1 (v/v) from the free pyranine derivative **Py-Ad** (solid line), the caged pyranine derivative **NPy-Ad** (dotted line), and the caged pyranine derivative **NPy-Ad** after illuminating with the LED at λ_{exc}=(365±25) nm (B: 2.5×10^{-8} E.s^{-1}, 1.4×10^{-3} E.m^{-2}.s^{-1}; D: 1.1×10^{-8} E.s^{-1}, 6.2×10^{-4} E.m^{-2}.s^{-1}; F: 5.1×10^{-9} E.s^{-1}, 2.8×10^{-4} E.m^{-2}.s^{-1}) up to the stabilization of the fluorescence signal (dashed line recorded after time t = 4000 s). *T* = 293 K.

Fig. S10 displays the impact of light intensity (ranging from (0.5-2.5) 10^{-8} $E.s^{-1}$ - (2.8-14) 10^{-4} $E.m^{-2}.s^{-1}$) on **NPy-Ad** uncaging in pH = 7.4 PBS buffer: acetonitrile 1:1 (v:v). We noticed that the drop of light intensity drives: (i) a change from a biexponential to a monoexponential time evolution of the fluorescence signal. The shortest retrieved characteristic time is essentially inversely proportional to the light intensity, which suggests that this characteristic time is associated to a photochemical step whereas the longer characteristic time retrieved from the biexponential fit remains essentially constant upon changing light intensity, which supports this characteristic time to be associated to a thermally-driven step; (ii) a decay of the contrast between the final and initial fluorescence signal from 12 to 7; (iii) an increase of the uncaging yield from 35 to 52%.

The mechanism of light-driven removal of the nitroveratryl photolabile protecting group involves a photoactivation step followed by several thermally-driven steps.[4] The observation that the shortest retrieved characteristic time is essentially inversely proportional to the light intensity suggests that the photoactivation step is rate-limiting in the considered range of light intensity. We retrieved 15.6±1.6 $m^2.mol^{-1}$ for the associated cross section σ for **NPy-Ad** in pH = 7.4 PBS buffer: acetonitrile 1:1 (v:v). In contrast, the longest retrieved characteristic time is tentatively associated with some deaggregation phenomenon since it occurs in the most hydrophilic acetonitrile-buffer mixtures only.

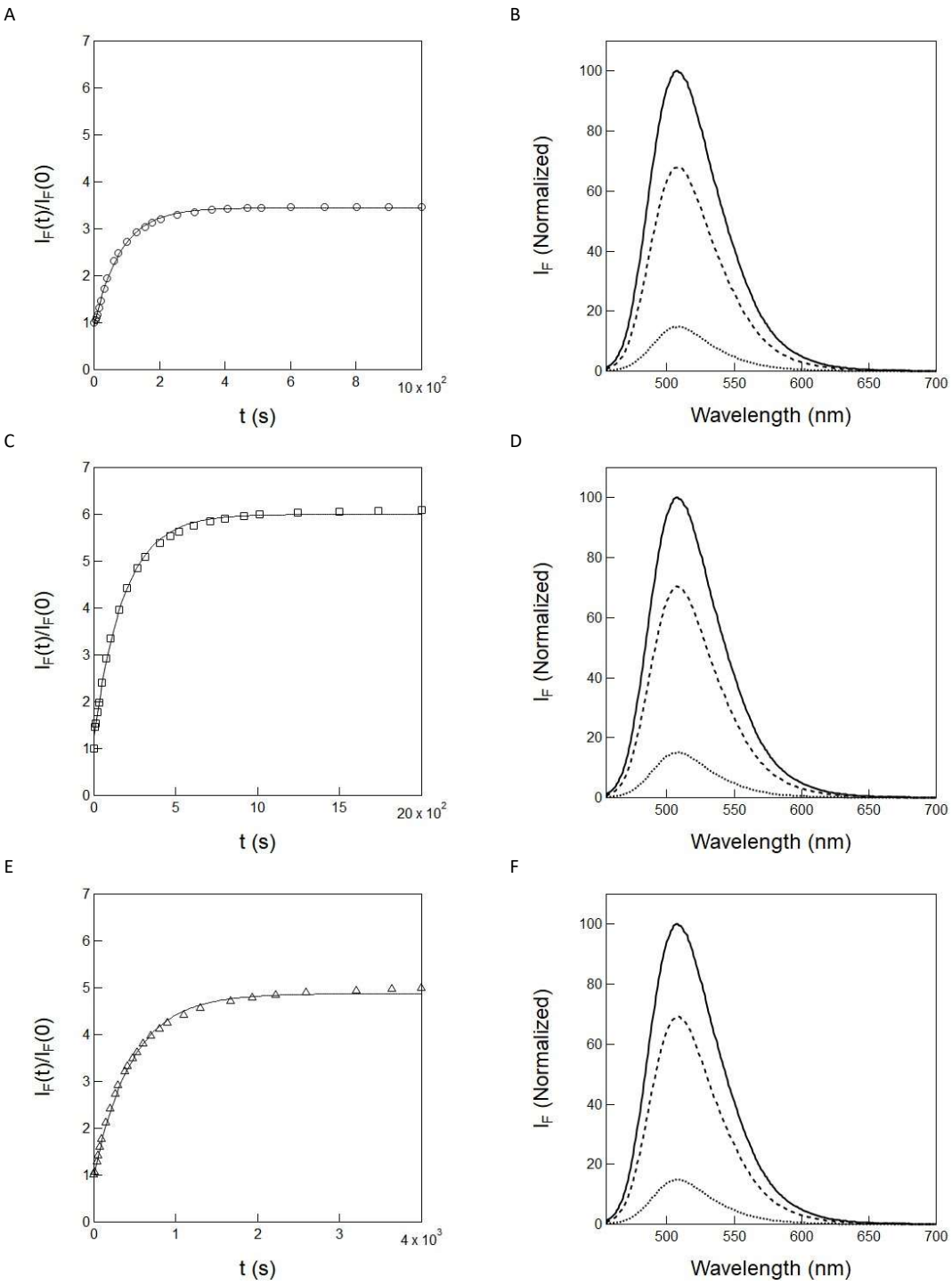

Fig. S11 A,C,E: *Preliminary evidence for uncaging in **NPy-S***. Temporal evolution of the fluorescence emission at λ_{em}= 500 nm upon homogeneous illumination of 2 μM ***NPy-S*** in 10 mM pH = 8.4 Trizma buffer contained in a 54 μL cuvette (3 mm optical pathlength) with the LED at λ_{exc}=(365±25) nm (A: 2.5×10^{-8} E.s^{-1}, 1.4×10^{-3} E.m^{-2}.s^{-1}; C: 1.1×10^{-8} E.s^{-1}, 6.2×10^{-4} E.m^{-2}.s^{-1}; E: 5.1×10^{-9} E.s^{-1}, 2.8×10^{-4} E.m^{-2}.s^{-1}). Markers: experimental data, solid line: monoexponential fit to Eq. (S1); the characteristic times τ = 82 s, τ = 184 s and τ = 468 s have been retrieved from A, C, and E respectively at *T* = 293 K; B,D,F: *Preliminary evaluation of the uncaging yield in **NPy-S***. Comparison of the fluorescence emission spectra recorded at a same 2 μM concentration in 10 mM pH = 8.4 Trizma buffer from the free pyranine derivative **HPTS** (solid line), the caged pyranine derivative ***NPy-S*** (dotted line), and the caged pyranine derivative ***NPy-S*** after illuminating with the LED at λ_{exc}=(365±25) nm (B: 2.5×10^{-8} E.s^{-1}, 1.4×10^{-3} E.m^{-2}.s^{-1}; D: 1.1×10^{-8} E.s^{-1}, 6.2×10^{-4} E.m^{-2}.s^{-1}; F: 5.1×10^{-9} E.s^{-1}, 2.8×10^{-4} E.m^{-2}.s^{-1}) up to the stabilization of the fluorescence signal (dashed line recorded after time *t*; B: *t* = 1000 s; D: *t* = 2000 s; F: *t* = 4000 s). *T* = 293 K.

Fig. S11 displays the impact of light intensity on uncaging the hydrophilic caged pyranine **NPy-S**. Upon illumination of **NPy-S** in 10 mM pH = 8.4 Trizma buffer at 365 nm, the fluorescence signal rises by a factor up to 6, which we evaluated to be associated to an uncaging yield of 56% from comparing the final signal with a reference **HPTS** solution at the same concentration in the same solvent. Moreover, the time fluorescence emission from the aqueous solution of **NPy-S** in 10 mM pH = 8.4 Trizma buffer is satisfactorily accounted by a monoexponential fit at light intensities ranging from 0.5 to 2.5 10^{-8} $E.s^{-1}$ ((2.8-14) 10^{-4} $E.m^{-2}.s^{-1}$). The retrieved characteristic time is essentially inversely proportional to the light intensity, which yields 8.4±0.7 $m^2.mol^{-1}$ for the associated uncaging cross section.

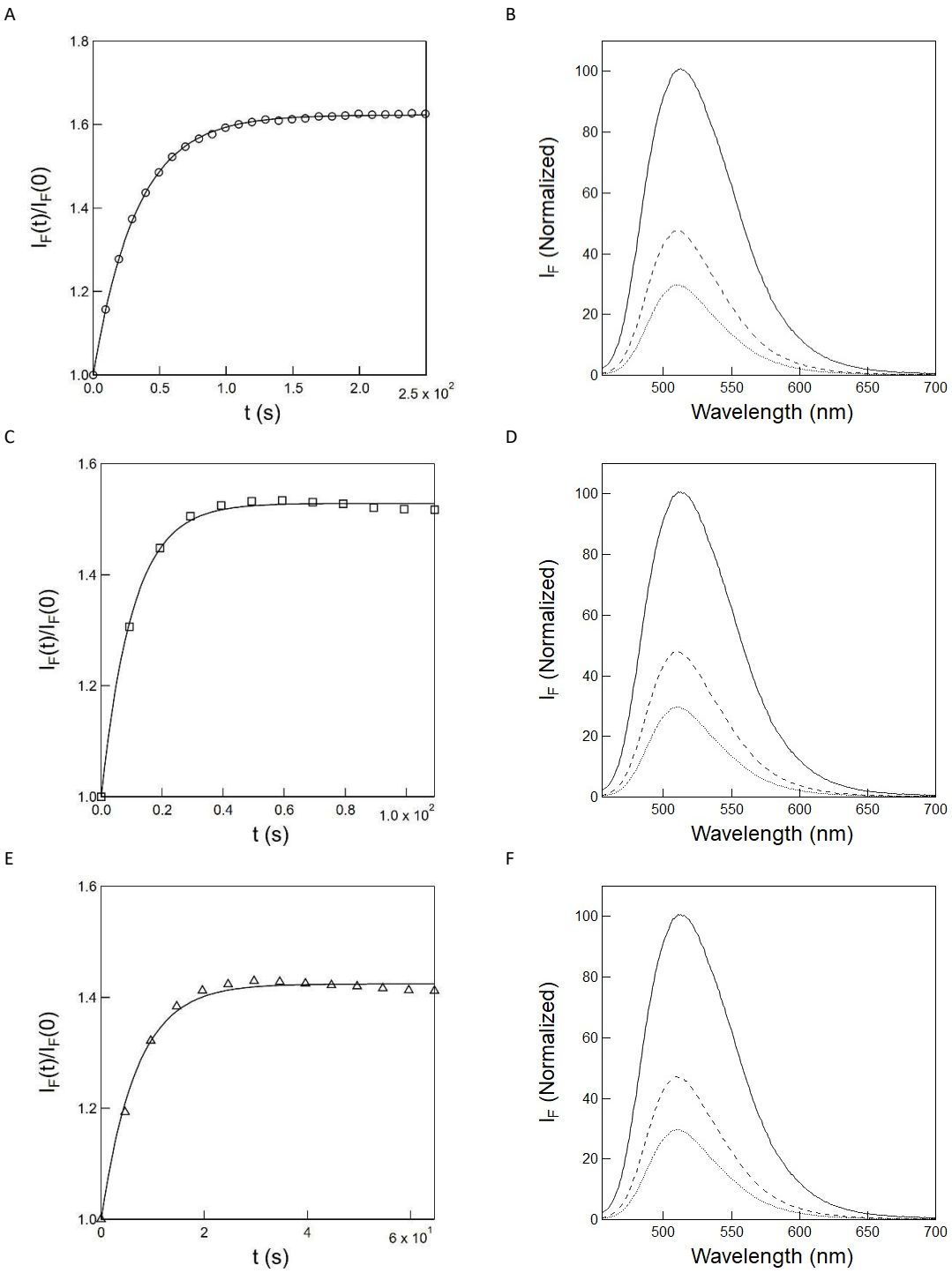

Fig. S12 A,C,E: *Preliminary evidence for uncaging in **CPy-S***. Temporal evolution of the fluorescence emission at λ_{em}= 510 nm upon homogeneous illumination of 2 µM **CPy-S** in 10 mM pH = 8.4 Trizma buffer contained in a 54 µL cuvette (3 mm optical pathlength) with the LED at λ_{exc}=(365±25) nm (A: 1.1 ×10^{-9} E.s^{-1}, 6.2 ×10^{-5} E.m^{-2}.s^{-1}; C: 2.6 ×10^{-9} E.s^{-1}, 1.4 ×10^{-4} E.m^{-2}.s^{-1}; E: 4.9 ×10^{-9} E.s^{-1}, 2.7 ×10^{-4} E.m^{-2}.s^{-1}). Markers: experimental data, solid line: exponential fit to Eq. (S1); The characteristic times τ = 33 s, τ = 10 s and τ = 7 s, have been retrieved from A, C, and E respectively at *T* = 293 K; B,D,F: Preliminary evaluation of the uncaging yield in **CPy-S**. Comparison of the fluorescence emission spectra recorded at a same 2 µM concentration in 10 mM pH = 8.4 Trizma buffer from the free pyranine derivative **HPTS** (solid line), the caged pyranine derivative **CPy-S** (dotted line), and the caged pyranine derivative **CPy-S** after illuminating with the LED at λ_{exc}=(365±25) nm (B: 1.1 ×10^{-9} E.s^{-1}, 6.2 ×10^{-5} E.m^{-2}.s^{-1}; D: 2.6 ×10^{-9} E.s^{-1}, 1.4 ×10^{-4} E.m^{-2}.s^{-1}; F: 4.9 ×10^{-9} E.s^{-1}, 2.7 ×10^{-4} E.m^{-2}.s^{-1}) up to the stabilization of the fluorescence signal (dashed line recorded after time t = 250 s). *T* = 293 K.

Fig. S12 displays the impact of light intensity on **CPy-S** uncaging. Upon illumination of **CPy-S** in 10 mM pH = 8.4 Trizma buffer at 365 nm, the fluorescence signal rises by a factor up to 2, which we evaluated to be associated to an uncaging yield higher than 17 % from comparing the final signal with a reference **HPTS** solution at the same concentration in the same solvent. Moreover, the time fluorescence emission from the aqueous solution of **CPy-S** in 10 mM pH = 8.4 Trizma buffer is satisfactorily accounted by a monoexponential fit at light intensities ranging from 1.1 to 4.9 10^{-9} $E.s^{-1}$ ((0.6-2.7) 10^{-4} $E.m^{-2}.s^{-1}$). The retrieved characteristic time is essentially inversely proportional to the light intensity, which yields 560±56 $m^2.mol^{-1}$ for the associated uncaging cross section σ.

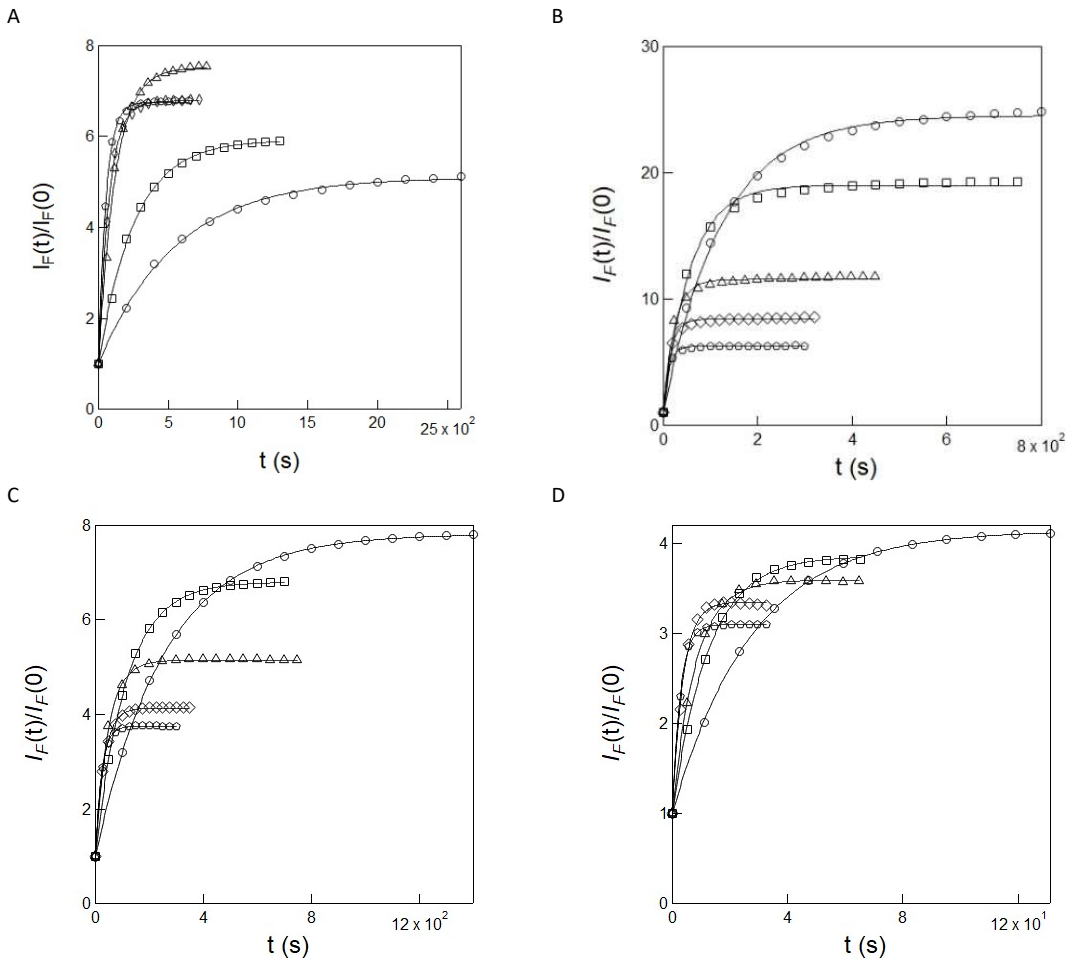

Fig. S13 *Measurement of the uncaging cross section of **NPy-Ab, NPy-Ad, NPy-S** and **CPy-S** at 365 nm.* A: Time evolution of the normalized fluorescence emission at 550 nm from 1 µM **NPy-Ab** in 10 mM pH = 8.4 Trizma buffer in a 54 µL cuvette (3 mm optical pathlength) upon irradiation at constant light intensity at 365 nm at various light intensities (in 10^{-9} E.s^{-1}): 6.5 (circles), 12.9 (squares), 25.9 (triangles), 38.1 (diamonds) and 51.7 (pentagons). Markers: Experimental data; Solid lines: Monoexponential fit with Eq. (S1); the characteristic time (s): 551, 257, 119, 76 and 54 have been retrieved at the corresponding light intensities; B: Time evolution of the normalized fluorescence emission at 540 nm from 2 µM **NPy-Ad** in 1 mM pH = 8.4 Trizma buffer/acetonitrile 1/19 (v/v) contained in a 54 µL cuvette (3 mm optical pathlength) upon irradiation at constant light intensity at 365 nm at various light intensities (in 10^{-9} E. s^{-1}): 6.0 (circles), 12.0 (squares), 23.9 (triangles), 35.9 (diamonds) and 47.9 (pentagons). Markers: Experimental data; Solid lines: Monoexponential fit with Eq. (S1); the characteristic times 119 s, 49 s, 18 s, 11 s and 8 s have been retrieved at the corresponding light intensities; C: Time evolution of the normalized fluorescence emission at 510 nm from 2 µM **NPy-S** in 10 mM pH = 8.4 Trizma buffer contained in a 54 µL cuvette (3 mm optical pathlength) upon irradiation at constant light intensity at 365 nm at various light intensities (in 10^{-9} E.s^{-1}): 6.0 (circles), 12.0 (squares), 23.9 (traingles), 35.9 (diamonds) and 47.9 (pentagons). Markers: Experimental data; Solid lines: Monoexponential fit with Eq. (S1); the characteristic times 257 s, 113 s, 46 s, 30 s and 20 s have been retrieved at the corresponding light intensities; D: Time evolution of the normalized fluorescence emission at 510 nm from 2 µM **CPy-S** in 10 mM pH = 8.4 Trizma buffer contained in a 54 µL cuvette (3 mm optical pathlength) upon irradiation at constant light intensity at 365 nm at various light intensities (in 10^{-9} E.s^{-1}): 1.2 (circles), 2.6 (squares), 4.9 (triangles), 11.2 (diamonds) and 15.1 (pentagons) . Markers: Experimental data; Solid lines: Monoexponential fit with Eq. (S1); the characteristic times 27 s, 12 s, 8 s, 4 s and 3 s have been retrieved at various light intensities. *T* = 293 K.

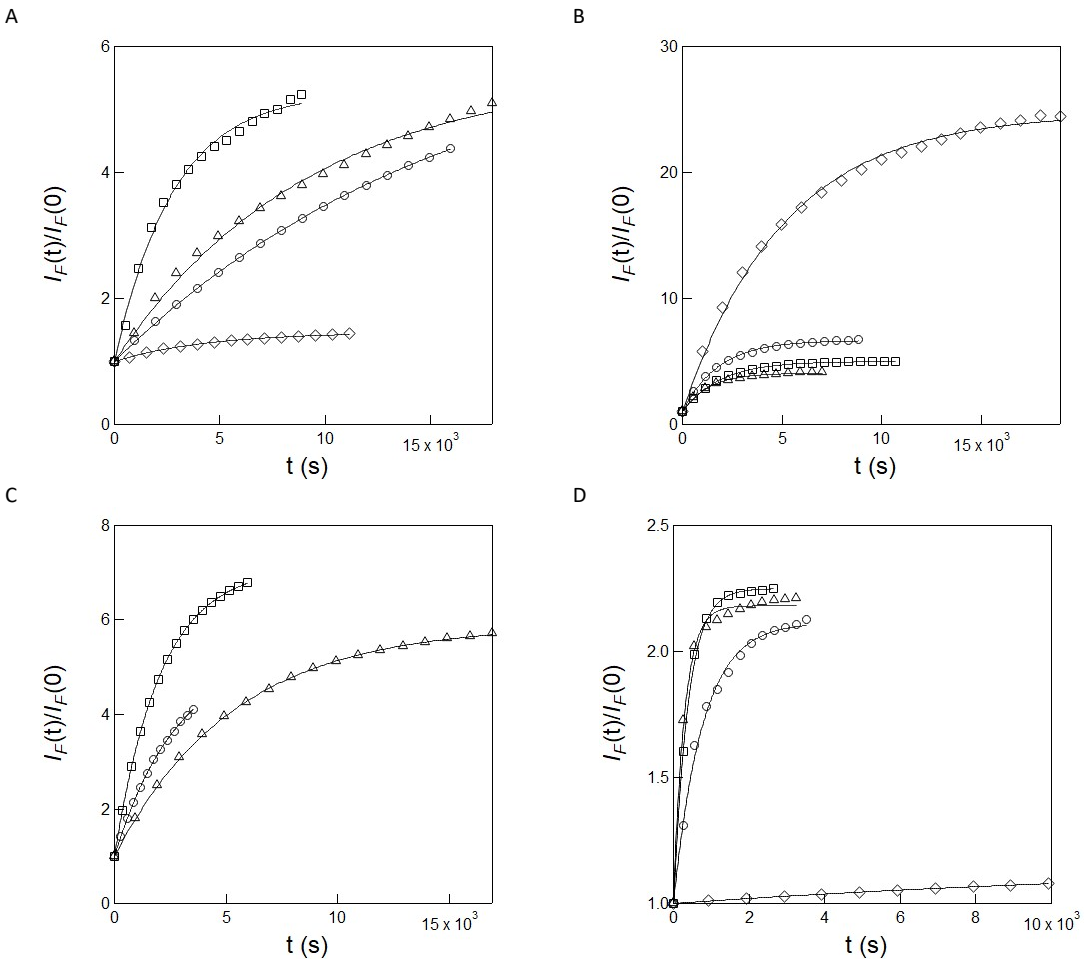

Fig. S14 *Measurement of the uncaging cross section of **NPy-Ab**, **NPy-Ad**, **NPy-S** and **CPy-S** at 300, 365, 405 and 440 nm.* A: Time evolution of the normalized fluorescence emission at 540 nm from 2 µM **NPy-Ab** in 10 mM pH = 7.4 PBS contained in a 1×1 cm^2 quartz cuvette upon irradiation at constant light intensity at 300 (circles), 365 (squares), 405 (triangles), and 440 (diamonds) nm at the following light intensities (in 10^{-5} E.m^{-2}.s^{-1}): 1.8, 4.3, 5.8, and 6.3 respectively. Markers: Experimental data; Solid lines: Monoexponential fit with Eq. (S1); the characteristic times 16360 s, 2820 s, 9370 s, and 4420 s have been retrieved at various excitation wavelength respectively from A. B: Time evolution of the normalized fluorescence emission at 540 nm from 2 µM **NPy-Ad** in 1 mM pH = 8.4 Trizma buffer/acetonitrile 1/19 (v/v) contained in a 1×1 cm^2 quartz cuvette upon irradiation at constant light intensity at 300 (circles), 365 (squares), 405 (triangles), and 440 (diamonds) nm at the following light intensities (in 10^{-5} E.m^{-2}.s^{-1}): 2.7, 6.5, 8.7, and 9.5 respectively. Markers: Experimental data; Solid lines: Monoexponential fit with Eq. (S1); the characteristic times 1760 s, 1800 s, 1210 s, and 5190 s have been retrieved at various excitation wavelength respectively from B. C: Time evolution of the normalized fluorescence emission at 510 nm from 2 µM **NPy-S** in 10 mM pH = 8.4 Trizma buffer contained in a 1×1 cm^2 quartz cuvette upon irradiation at constant light intensity at 300 (circles), 365 (squares), and 405 (triangles) nm at the following light intensities (in 10^{-5} E.m^{-2}.s^{-1}): 6.2, 15, and 20 respectively. Markers: Experimental data; Solid lines: Monoexponential fit with Eq. (S1); the characteristic times 2820 s, 2070 s and 5350 s have been retrieved at various excitation wavelength respectively from C. D: Time evolution of the normalized fluorescence emission at 510 nm from 2 µM **CPy-S** in 10 mM pH = 8.4 Trizma buffer contained in a 1 cm quartz cuvette upon irradiation at constant light intensity at 300 (circles), 365 (squares), 405 (triangles) and 440 (diamonds) nm at the following light intensities (in 10^{-6} E.m^{-2}.s^{-1}): 1.0, 2.4, 3.2 and 1.7 respectively. Markers: Experimental data; Solid lines: Monoexponential fit with Eq. (S1); the characteristic times 763 s, 385 s, 294 s and 12578 s have been retrieved at various excitation wavelength respectively from D. T = 293 K.

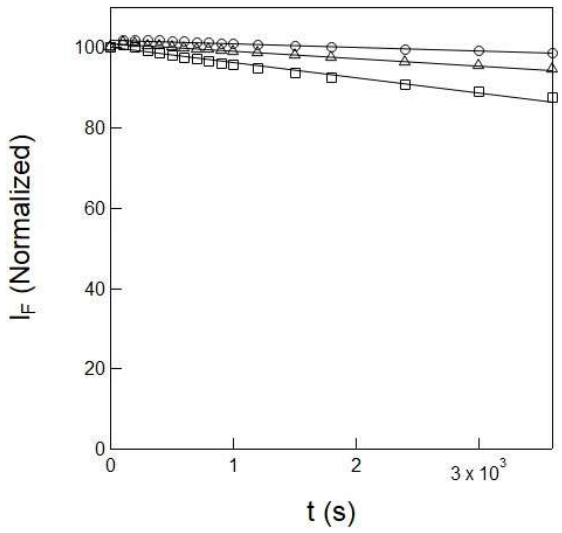

Fig. S15 *Photostability of **Py-Ab**, **Py-Ad** and **HPTS**.* Time evolution of the normalized fluorescence emission from 2 μM solution of **Py-Ab** (λ_{em}= 540 nm; circles) in 10 mM pH 7.4 PBS**, Py-Ad** (λ_{em}= 540 nm; squares) in 1 mM pH = 8.4 Trizma buffer/acetonitrile 1/19 (v/v), and **HPTS** (λ_{em}= 500 nm; triangles) in 10 mM pH = 8.4 Trizma buffer contained in a 54 μL cuvette (3 mm optical pathlength) upon homogeneous illumination with the LED at λ_{exc}=(365±25) nm (2.5×10^{-8} E.s^{-1}, 1.4×10^{-3} E.m^{-2}.s^{-1}) at the following times (s): 0, 100, 200, 300, 400, 500, 600, 700, 800, 900, 1000, 1200, 1500, 1800, 2400, 3000 and 3600. Markers: Experimental data, lines: linear fit. The extracted slopes are -8.3×10^{-4}, -3.7×10^{-3}, and -1.8×10^{-3} s^{-1} and the characteristic times 1205, 270, and 555 s have been retrieved from the slopes of the linear fit for **Py-Ab**, **Py-Ad** and **HPTS** respectively. *T* = 293 K.

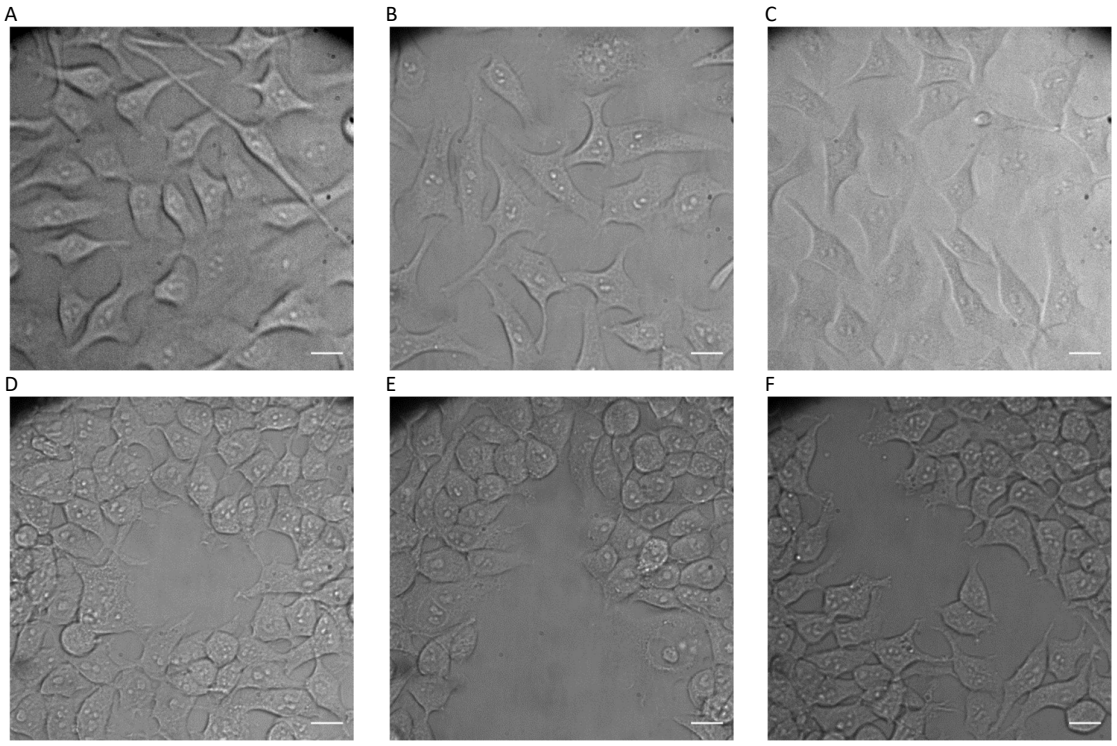

Fig. S16 *Bright field images of living Hela (A-C) and HEK (D-F) cells*. The cells were conditioned with DMEM (A,D), 0.5 µM (B,E), and 1 µM (C,F) **NPy-Ab** for 30 min (scale bar: 20 µm). *T* = 298 K.

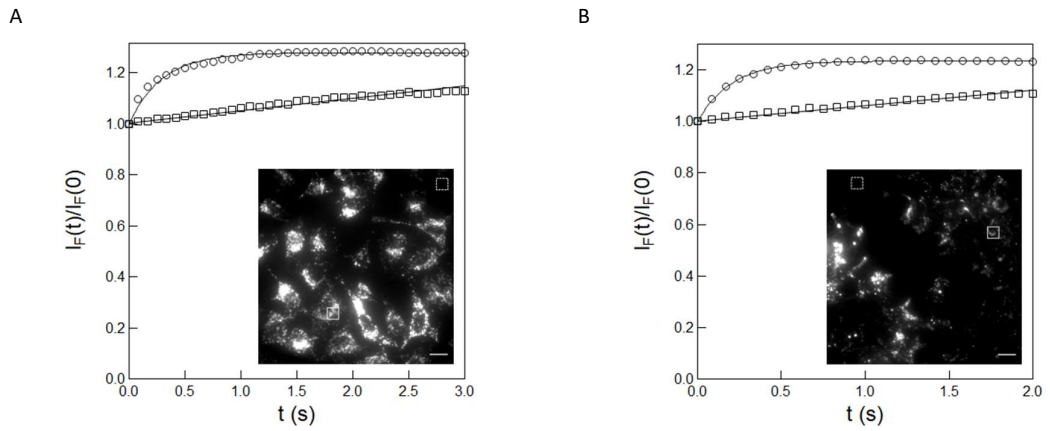

Fig. S17 *Measurement of the photon flux density in living Hela and HEK cells at 405 nm in epifluorescence microscopy*. Time evolution of the fluorescence signal from living Hela (A) and HEK (B) cells (**inset;** scale bar: 20 µm) conditioned with 1 µM **NPy-Ab u**nder illumination at 405 nm. Markers: the circles and squares are associated with the frames delimited by the solid and dashed lines in the inset images respectively. Fluorescence signal as extracted from integrating the fluorescence level over the ROIs; Solid lines: Monoexponential fit with Eq. (S1); the characteristic times 0.28 and 0.21 s have been retrieved from processing the fluorescence signal over the frames delimited by the solid lines in A and B respectively. *T* = 298 K.

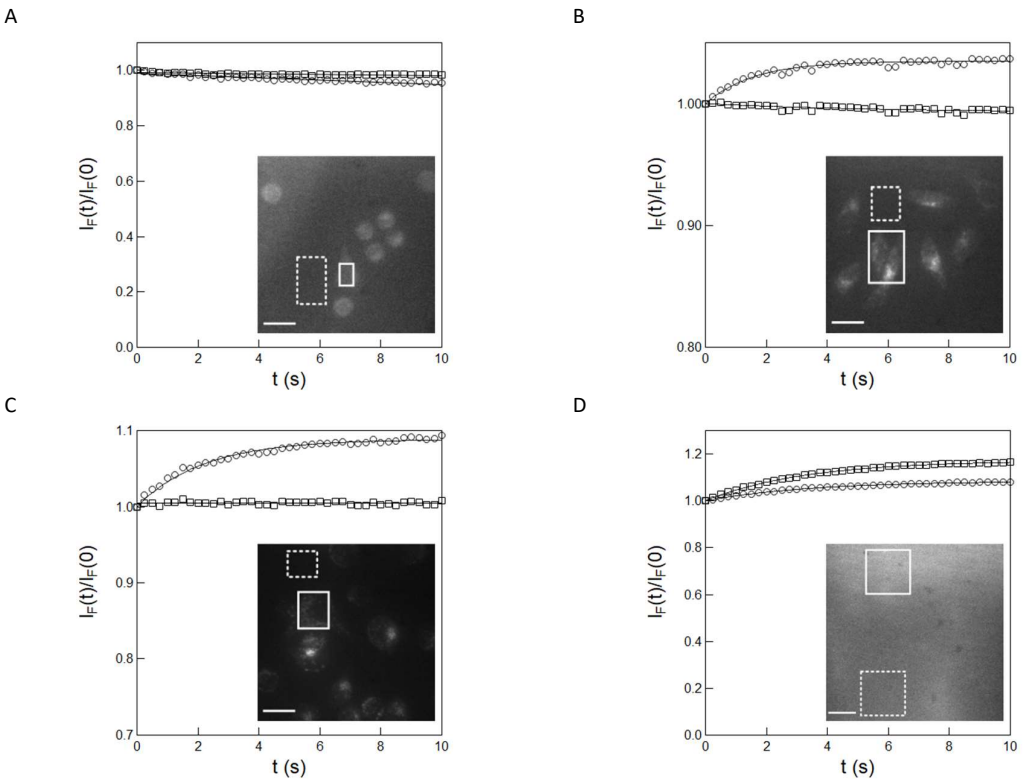

Fig. S18 *Measurement of the photon flux density in living Hela cells at 365 nm in epifluorescence microscopy.* Time evolution of the fluorescence signal from living Hela cells (**inset;** scale bar: 20 µm) conditioned with 1 µM **NPy-Aa** (A), 1 µM (B) and 0.5 µM (C) **NPy-Ab** and from the surrounding pH 7.4 PBS buffer (0.01 M phosphate, 0.154 M NaCl) under illumination at 365 nm; D: Time evolution of the fluorescence signal at 365 nm and images (**inset**) of 1 µM **NPy-Ab** solution in pH 7.4 PBS buffer under illumination at 365 nm. Markers: the circles and squares are associated with the frames delimited by the solid and dotted lines in the inset images respectively. Fluorescence signal as extracted from integrating the fluorescence level over the ROIs; Solid lines: Monoexponential fit with Eq. (S1); the characteristic times 1.6, 2.2 s have been retrieved from processing the fluorescence signal over the frames delimited by the solid line in B and C, whereas 3.2 and 3.4 s have been retrieved from processing the fluorescence signal over the frames delimited by the solid and dotted lines in D respectively. *T = 293 K*.

In addition to the measurement of light intensity at 405 nm in cultured cells reported in Figure 5 of the Main Text, we implemented the caged pyranine derivatives **NPy-Aa** and **NPy-Ab** for measuring light intensity in cultured cells at 365 nm. Living Hela living cells were conditioned for 1 h with 1 µM solutions of **NPy-Aa** and **NPy-Ab** in pH 7.4 PBS buffer (0.01 M phosphate, 0.154 M NaCl). Their external medium was subsequently washed prior to illumination to avoid any possible interference, which could originate from photoreleasing the free fluorophore in the incubating solution. Then the Hela cells were imaged with an epifluorescence by using 365 nm LED illumination. Fig. S18 displays the results. As shown in Fig. S18A, 365 nm illumination of the conditioned cells does not promote any rise of the fluorescence emission. In fact, the time evolution of the fluorescence signal is essentially similar to the behavior observed upon illuminating the background. This behavior suggests that the caged pyranine derivative **NPy-Aa** does not cross the cell membranes so as to be discarded for its use in biological media. In contrast, Fig. S18B,C shows that illumination at 365 nm of the cells conditioned with the caged pyranine **NPy-Ab** causes an increase of the fluorescence signal, which significantly departs from the corresponding behavior observed in the background. Moreover, we observed that the characteristic times retrieved from processing the fluorescence increase with a monoexponential function from illuminated cells and **NPy-Ab** solution in pH 7.4 PBS buffer under identical illuminations conditions were essentially similar (compare Fig. S18B,C and Fig. S18D). Hence, we could adopt the uncaging cross section of **NPy-Ab** in pH 7.4 PBS buffer to extract the value of the photon flux density applied on cells and found 0.1 $E.m^{-2}.s^{-1}$.

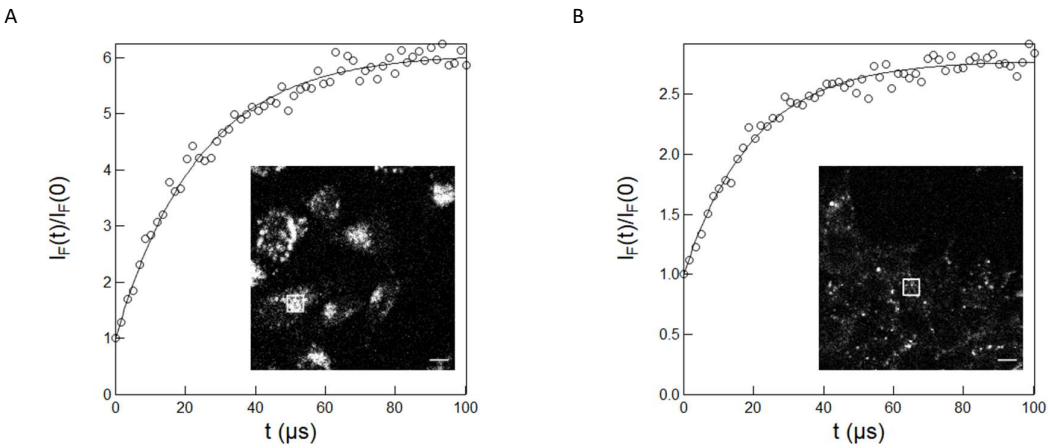

Fig. S19 *Measurements of light intensities in living Hela and HEK cells at 405 nm in confocal microscopy*. Time evolution of the fluorescence signal at 405 nm (laser power: 2%; frame: 256×256 pixel^2; zoom factor: 4; dwell time: 1.7 µs) and fluorescence image (**inset**; scale bar: 10 µm) of living Hela (A) and HEK (B) cells conditioned with 0.5 µM **NPy-Ab** (together with 2 µM DMSO originating from the **NPy-Ab** stock solution) in DMEM. Markers: Fluorescence signal as extracted from integrating the fluorescence level over the ROI (white frame in the inset image; Solid lines: Monoexponential fit with Eq. (S1); the characteristic times 24 and 20 µs have been retrieved from processing the fluorescence signal over the white frame in A and B respectively. *T* = 293 K.

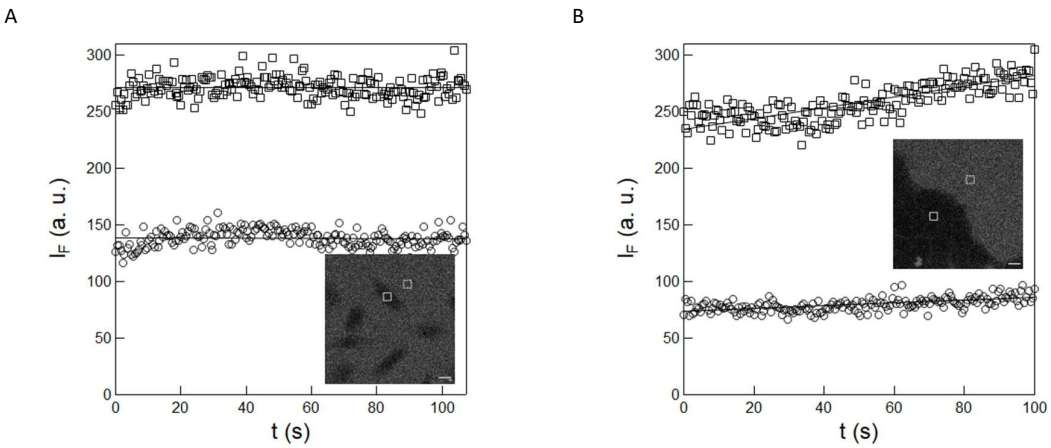

Fig. S20 *Permeation kinetics of **Py-Ab** in living Hela and HEK cells*. Time evolution of the fluorescence signal at 405 nm (laser power: 2%; frame: 512×512 pixel^2; zoom factor: 4; dwell time: 2.06 µs) and fluorescence image (**inset**; scale bar: 10 µm) of living Hela (A) and HEK (B) cells conditioned with 1 µM **Py-Ab** (together with 2 µM DMSO originating from the **Py-Ab** stock solution) in DMEM (the circles and squares markers are associated with the frames delimited by the solid and dotted lines in the inset image). *T* = 293 K.

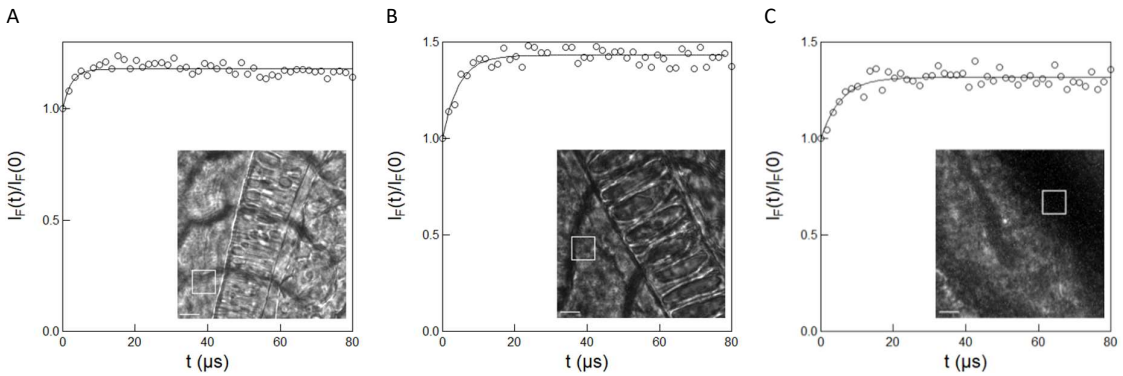

Fig. S21 *Measurement of the photon flux density delivered by a confocal microscope at 405 nm in living zebrafish embryos*. A,B,C: Time evolution of the fluorescence signal at 405 nm (laser power: 10%; frame: 256×256 pixel^2, zoom factor: 5; dwell time: 1.7 µs) and bright field image (**inset**; scale bar: 10 µm) of living zebrafish embryos conditioned with 0.1 µM (A), 1 µM (B) and 2 µM (C) of **NPy-Ab** in water (regions of interest - ROI: white frames). Markers: Fluorescence signal as extracted from integrating the fluorescence level over the ROIs; Solid lines: Monoexponential fit with Eq. (S1); the characteristic time 2.3, 4.5, and 5.5 µs has been retrieved from processing the fluorescence signal over the white frame in A, B and C respectively. *T* = 293 K.

NMR Spectra

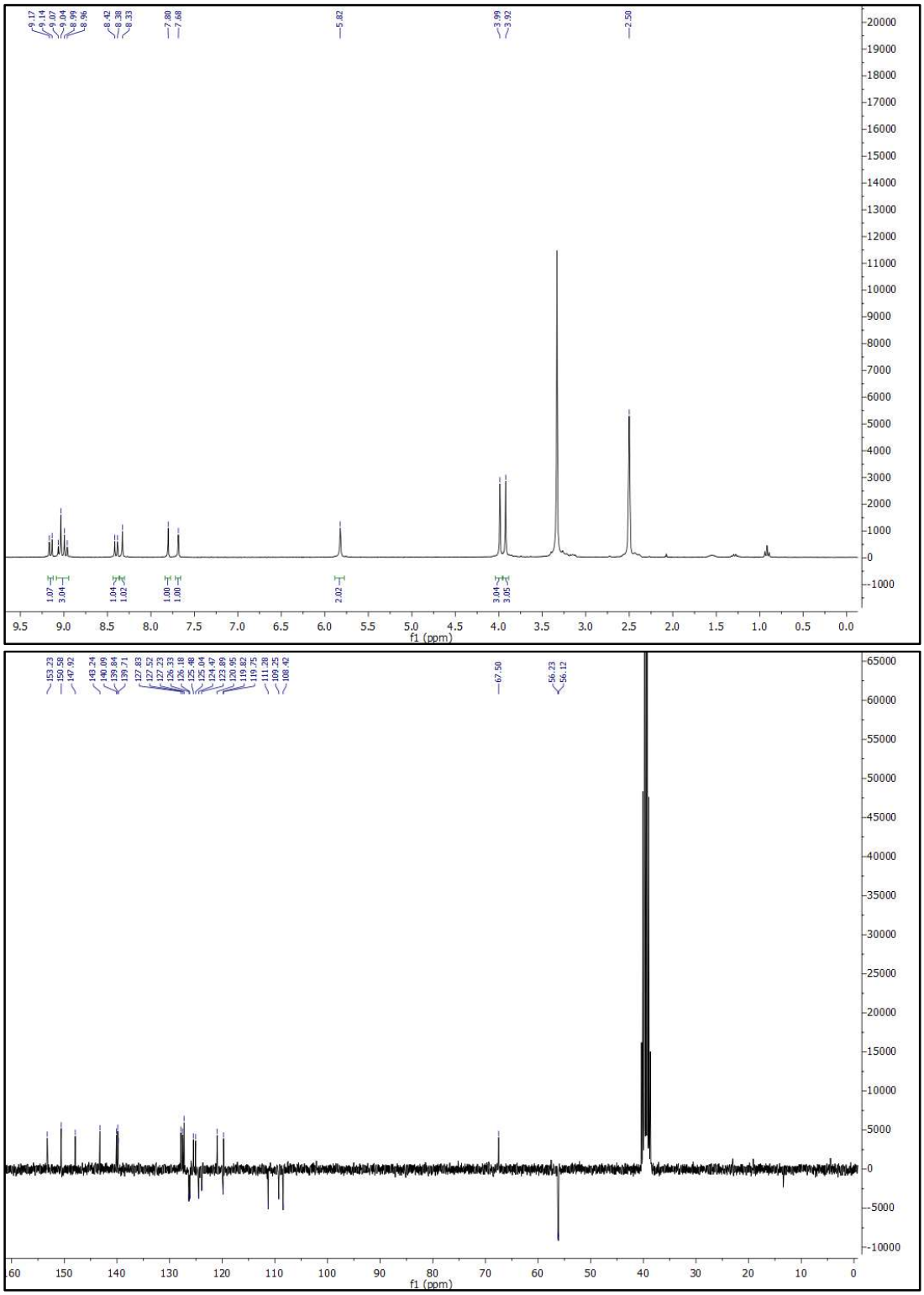

Fig. S22 ^{1}H and ^{13}C NMR spectra of **NPy-S**.

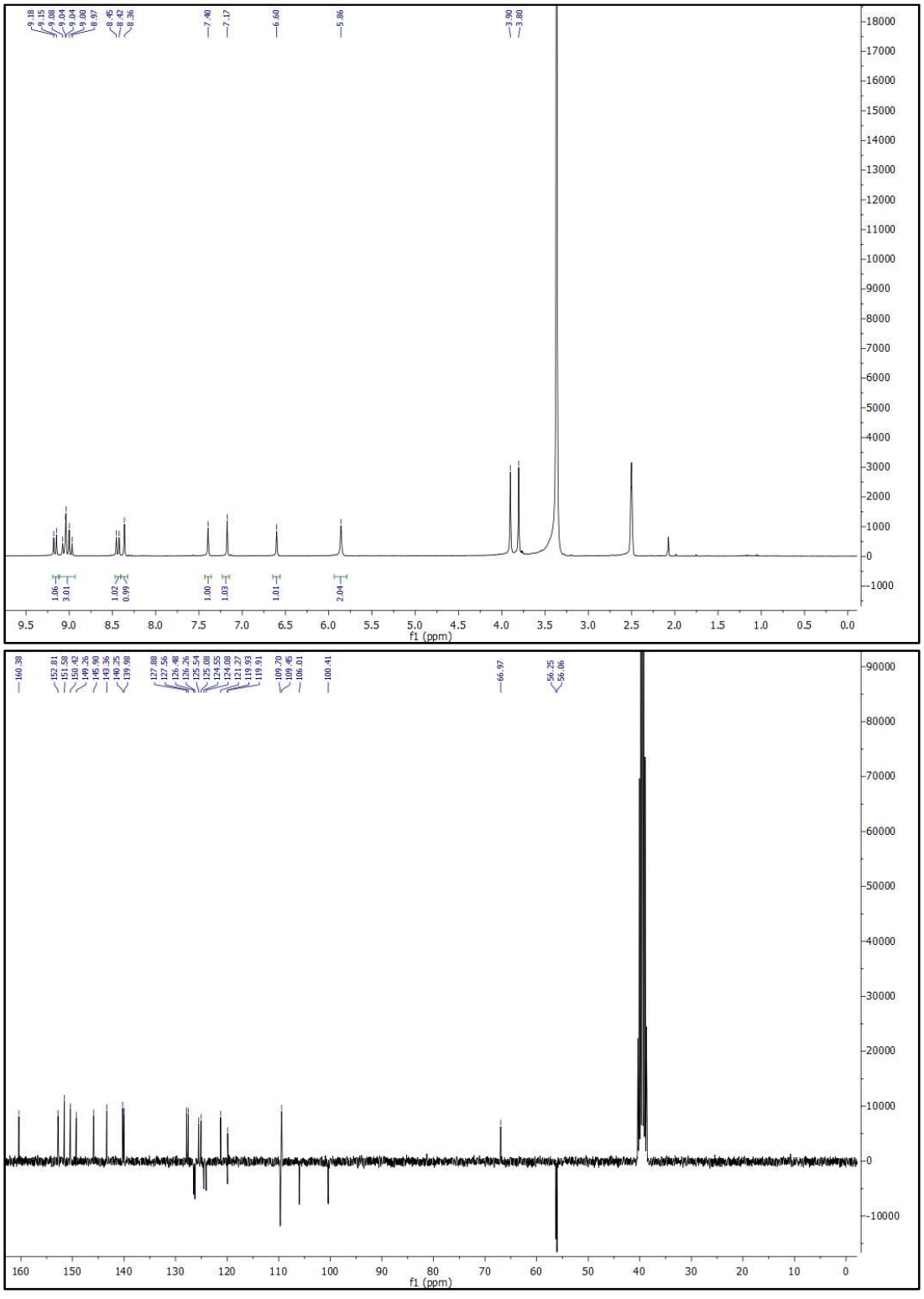

Fig. S23 ^{1}H and ^{13}C NMR spectra of **CPy-S**.

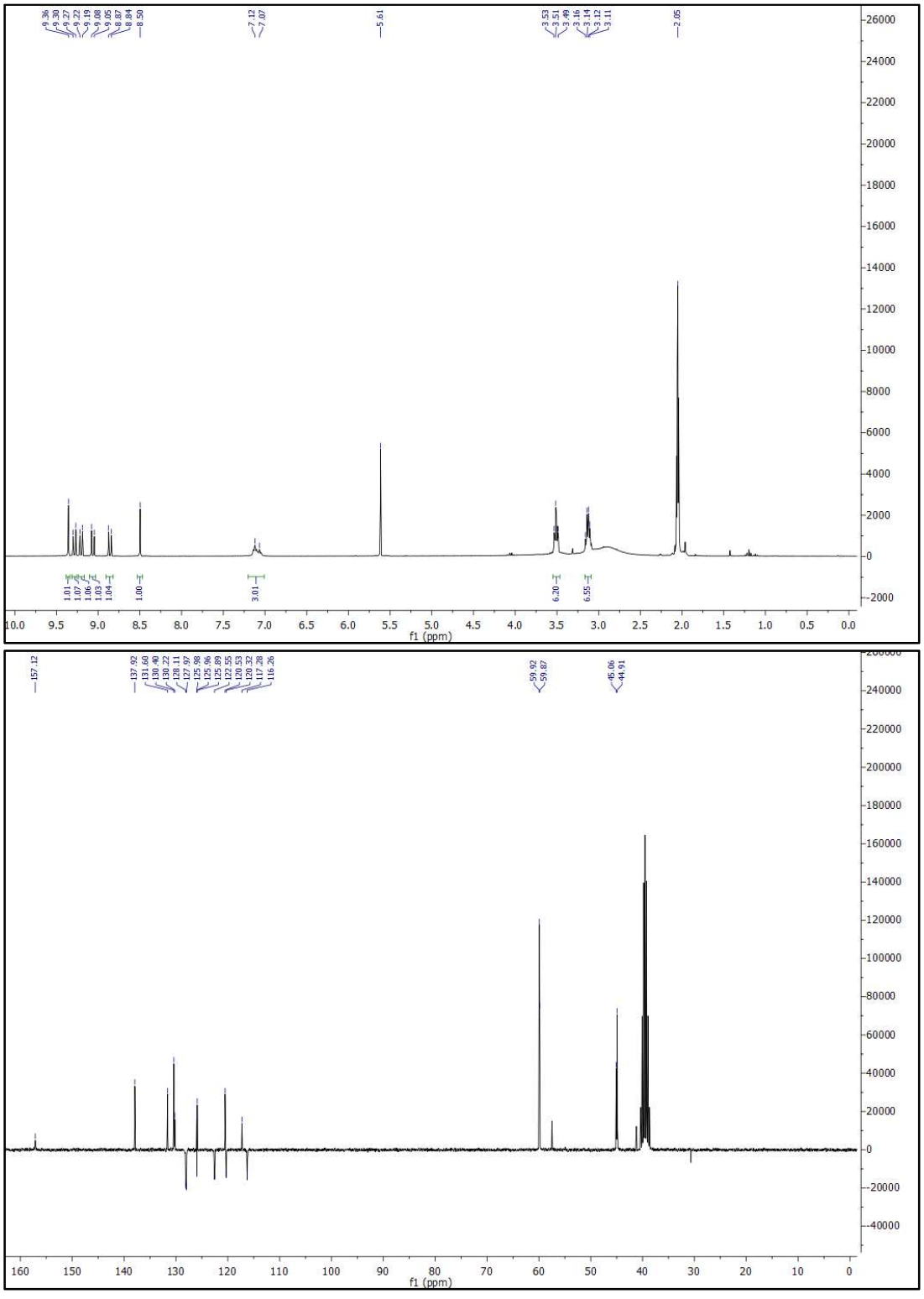

Fig. S24 ^{1}H and ^{13}C NMR spectra of **Py-Aa**.

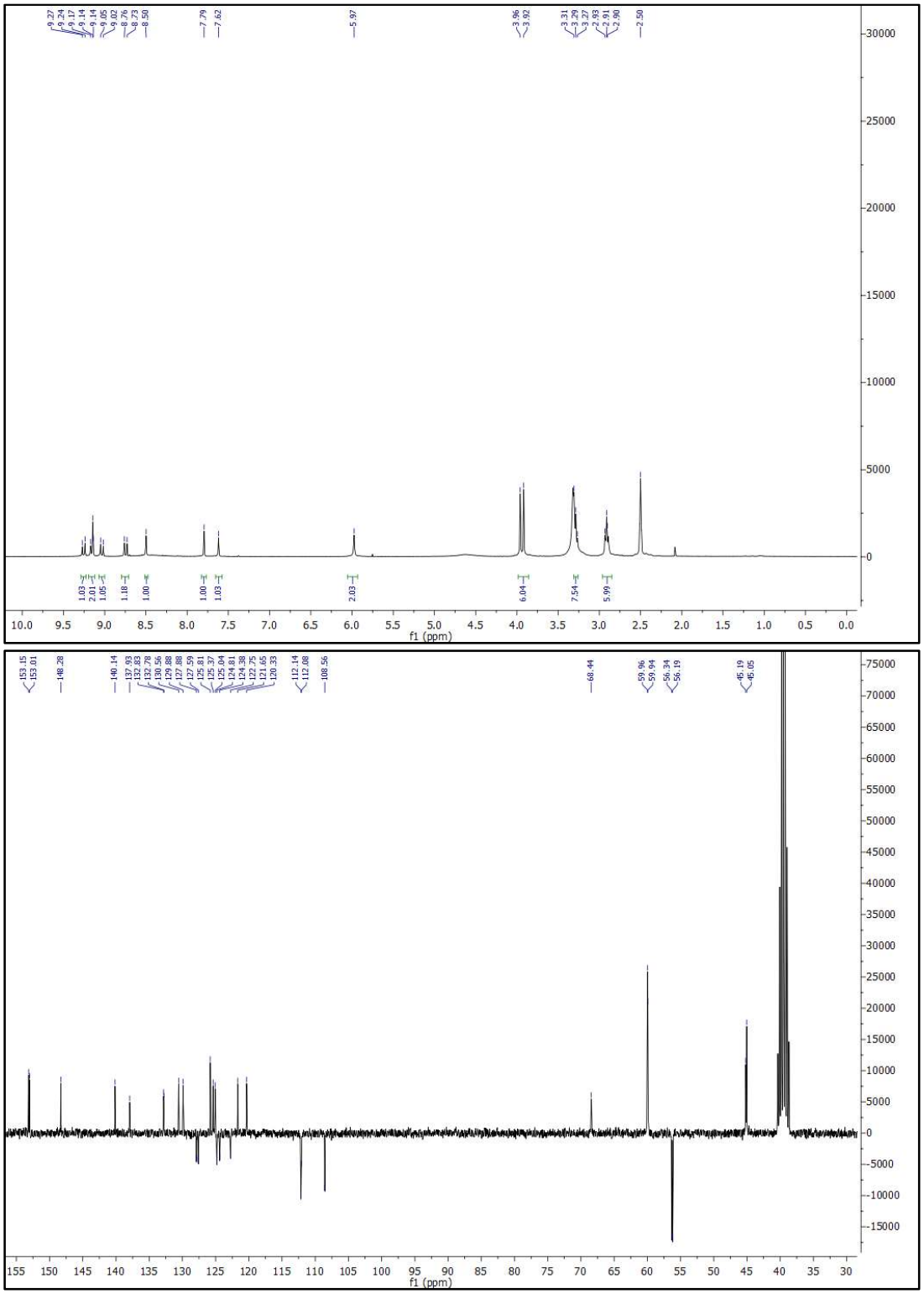

Fig. S25 ^{1}H and ^{13}C NMR spectra of **NPy-Aa**.

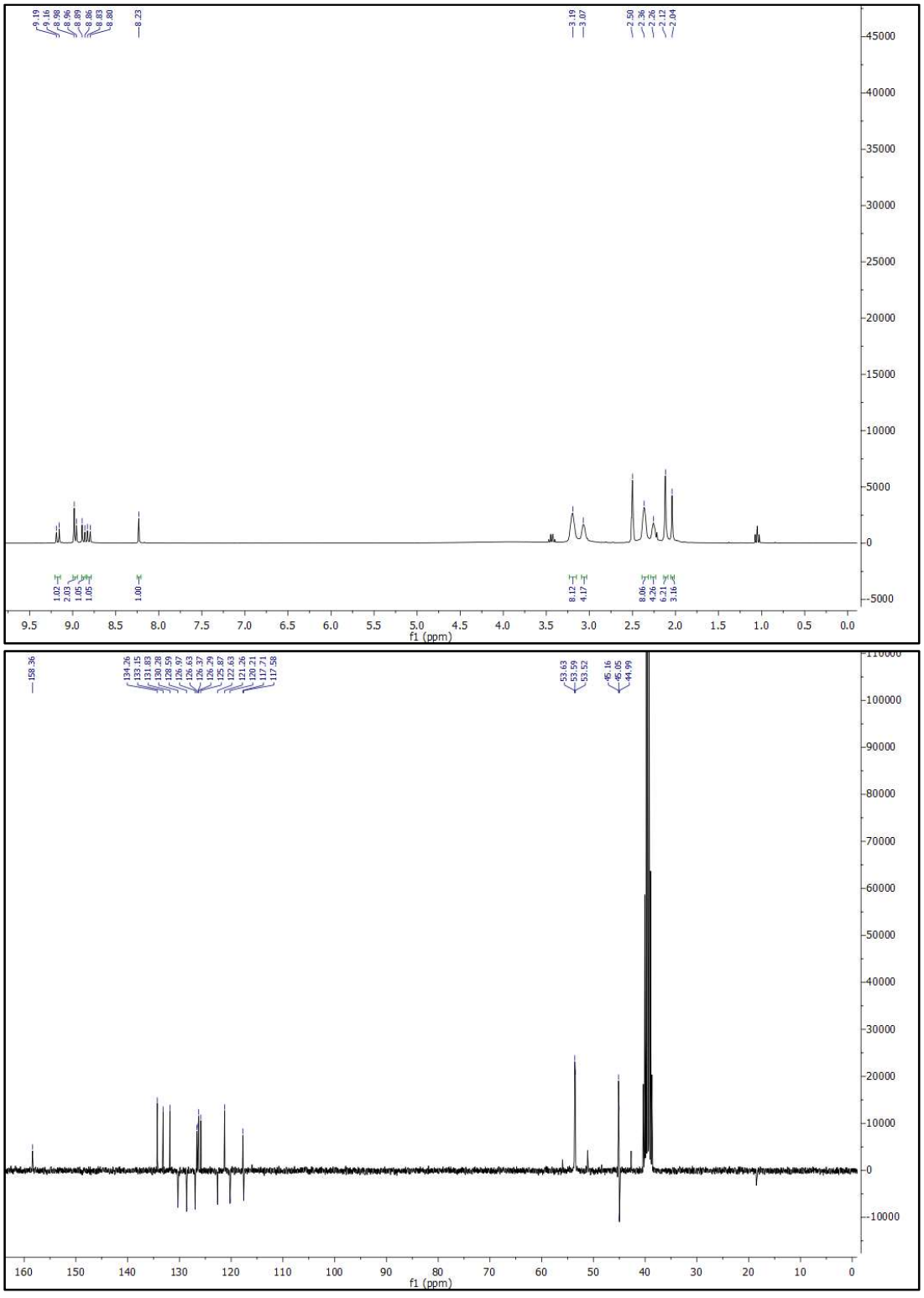

Fig. S26 ^{1}H and ^{13}C NMR spectra of **Py-Ab**.

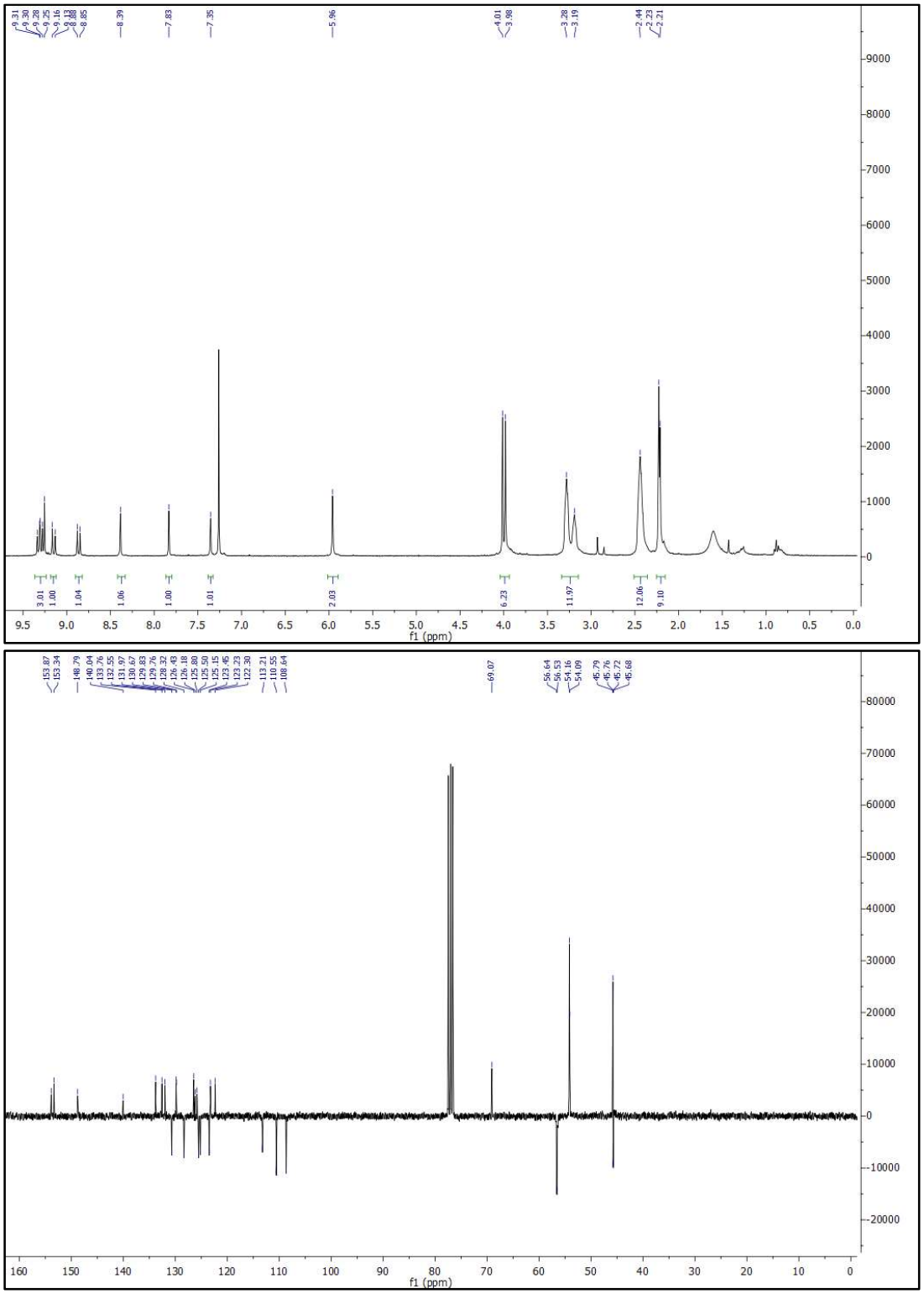

Fig. S27 ^{1}H and ^{13}C NMR spectra of **NPy-Ab**.

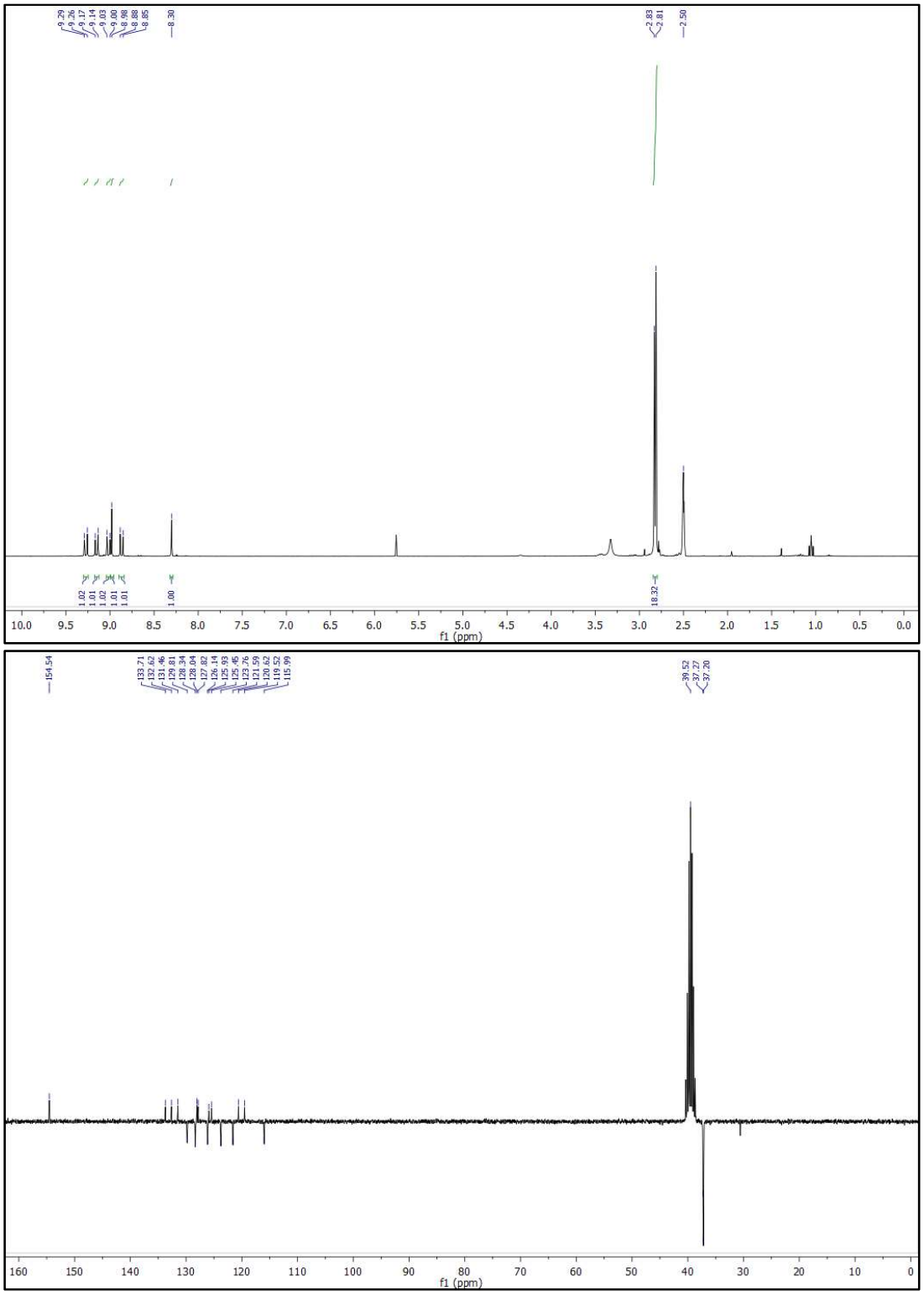

Fig. S28 ^{1}H and ^{13}C NMR spectra of **Py-Ac**.

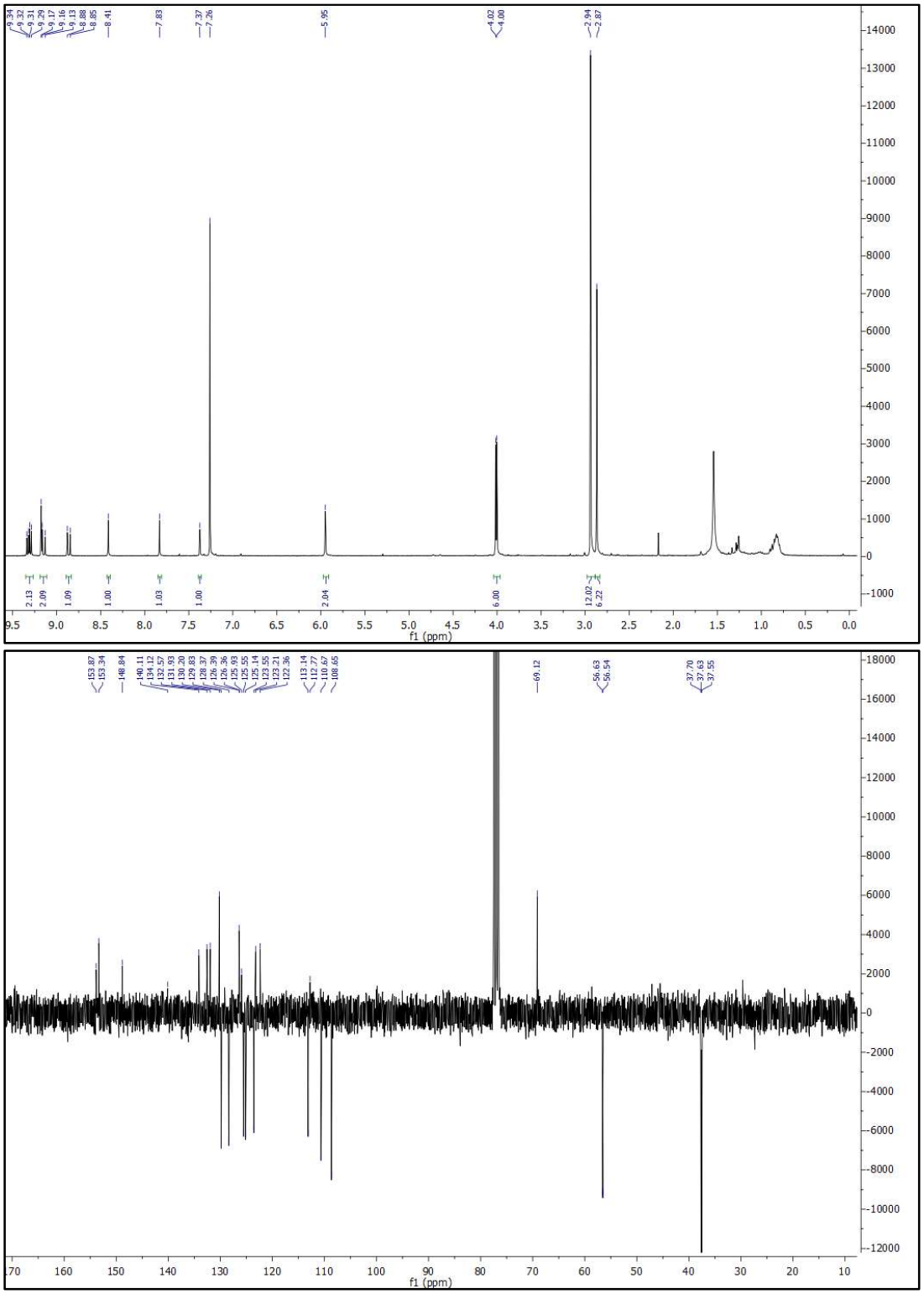

Fig. S29 ^{1}H and ^{13}C NMR spectra of **NPy-Ac**.

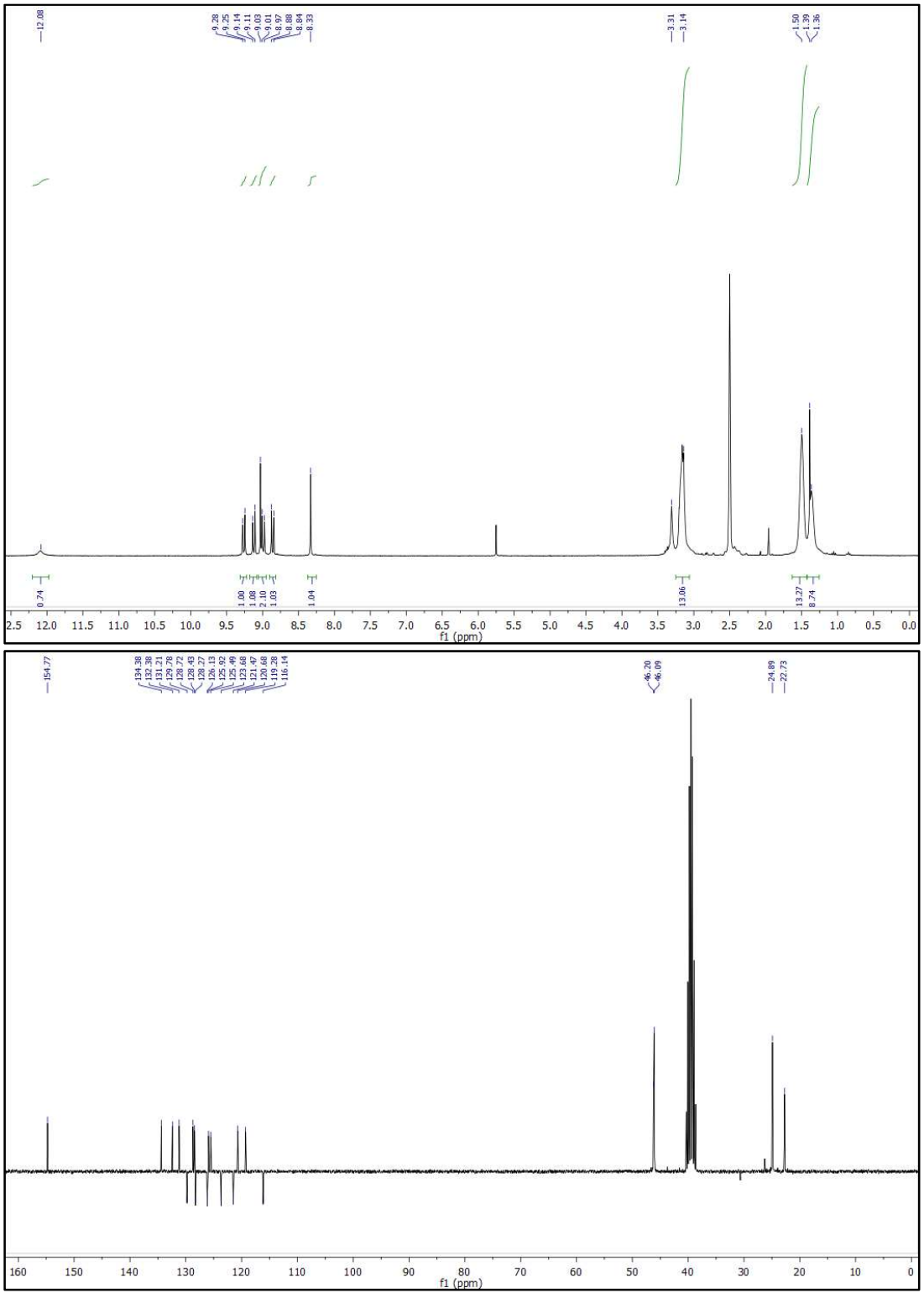

Fig. S30 ^{1}H and ^{13}C NMR spectra of **Py-Ad**.

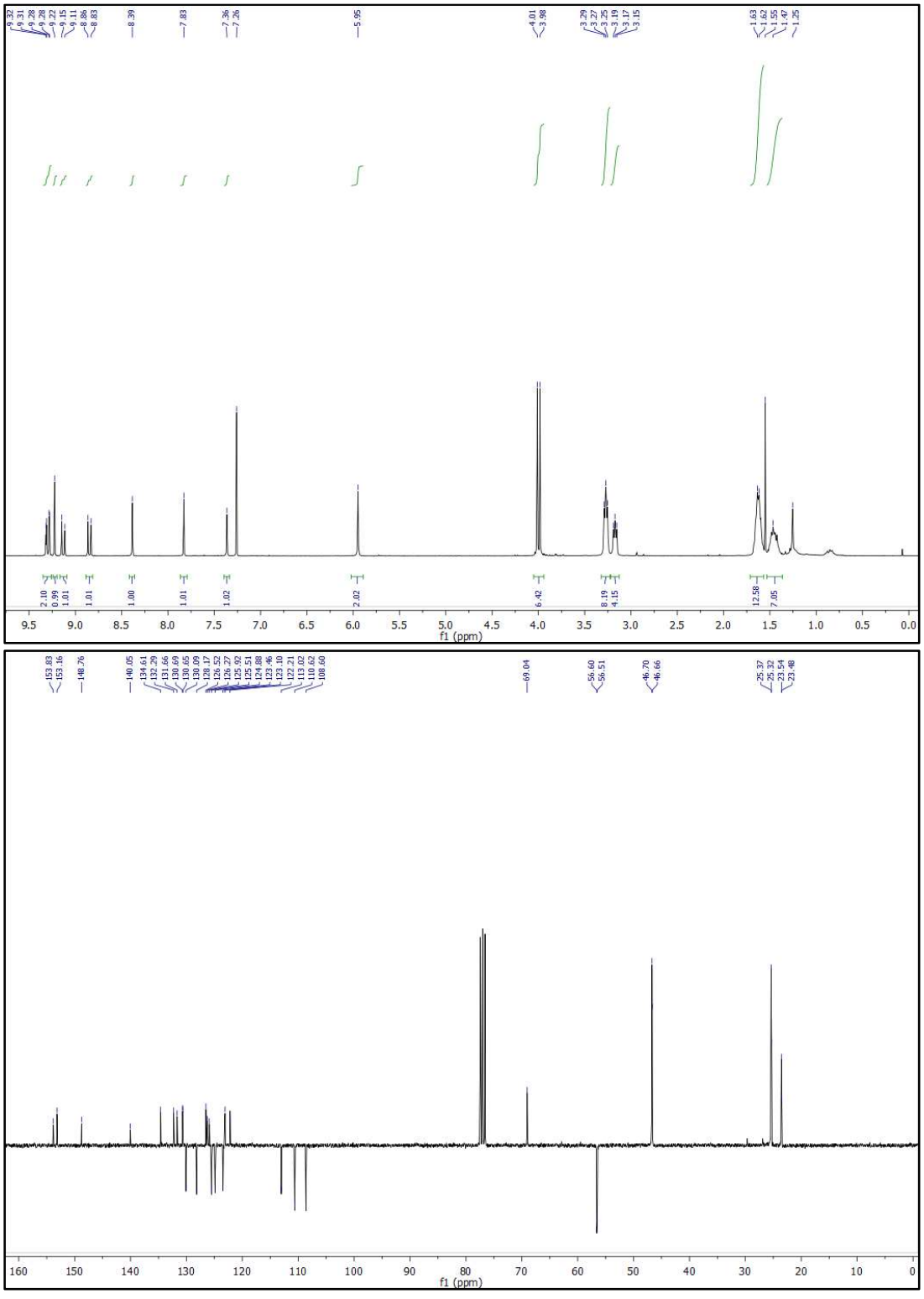

Fig. S31 ^{1}H and ^{13}C NMR spectra of **NPy-Ad**.

HPLC chromatograms

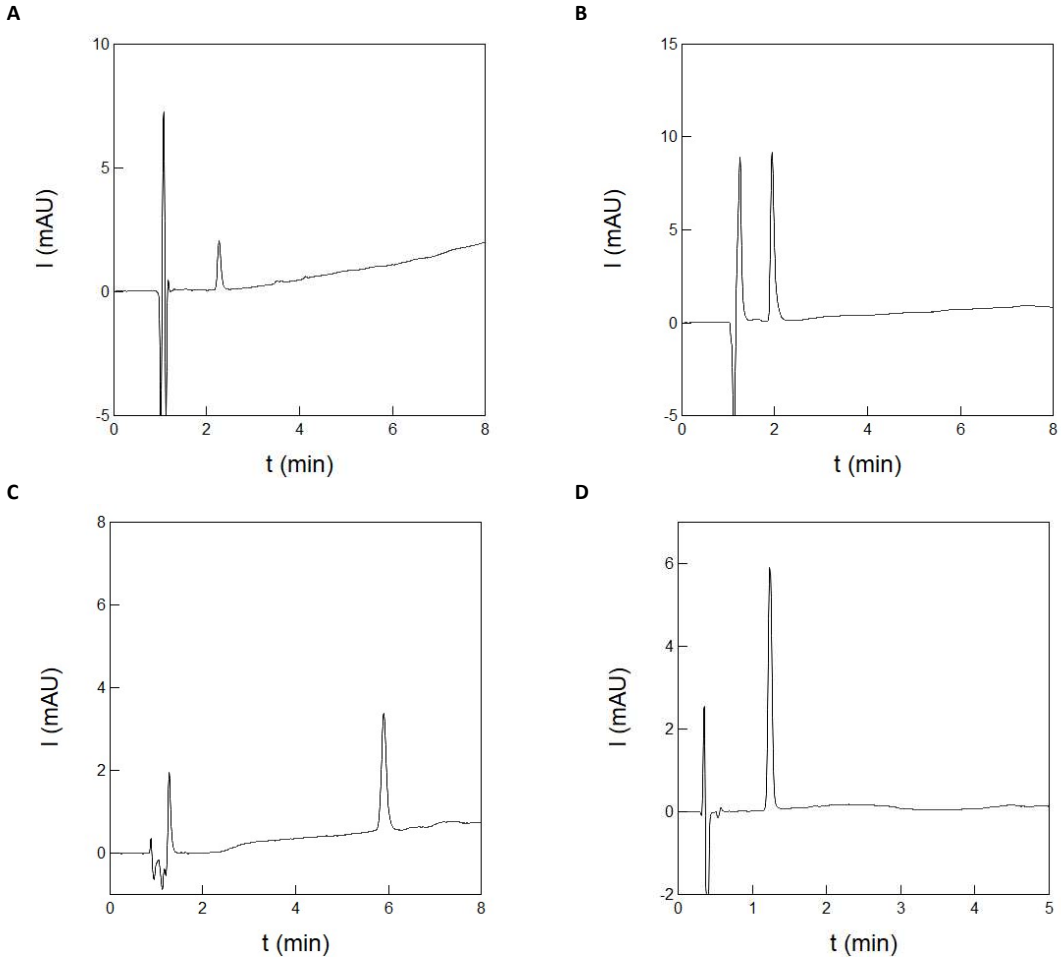

Fig. S32 *HPLC chromatograms of the free pyranine derivatives*. HPLC traces of **Py-Aa** (A), **Py-Ab** (B), **Py-Ad** (C), **HPTS** (D). The spectra were recorded from 2 μM solution in 10 mM pH 7.4 PBS (for **Py-Aa-b**), 1 mM pH = 8.4 Trizma buffer/acetonitrile 1/19 (v/v) (for **Py-Ad**), and 10 mM pH = 8.4 Trizma buffer (for **HPTS**). *T* = 293 K.

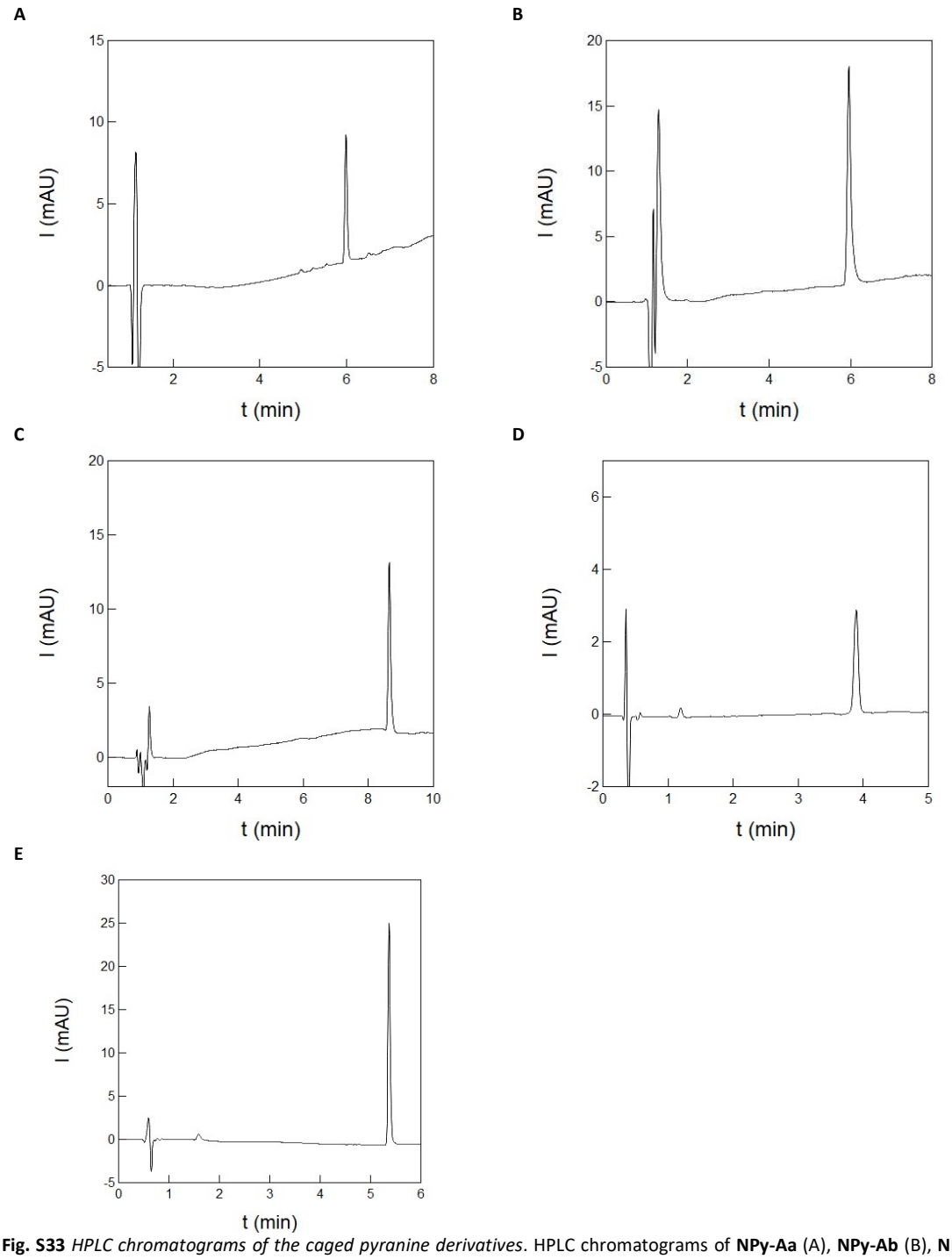

Fig. S33 *HPLC chromatograms of the caged pyranine derivatives*. HPLC chromatograms of **NPy-Aa** (A), **NPy-Ab** (B), **NPy-Ad** (C), **NPy-S** (D) and **CPy-S** (E). The spectra were recorded from 2 µM solution in 10 mM pH 7.4 PBS (for **NPy-Aa-b**), 1 mM pH = 8.4 Trizma buffer/acetonitrile 1/19 (v/v) (for **NPy-Ad**), and 10 mM pH = 8.4 Trizma buffer (for **NPy-S** and **CPy-S**). *T* = 293 K.

CE electropherogram

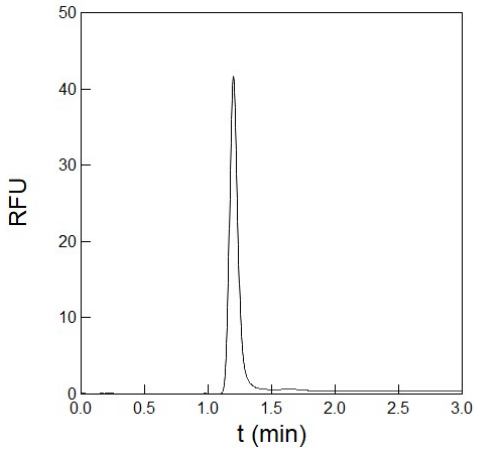

Fig. S34 *Capillary electrophoresis (CE) of the free pyranine derivative* ***Py-Ab***. The CE electropherogram was obtained from injecting a 0.25 µM solution of **Py-Ab** in 10 mM pH 8.4 Trizma buffer. *T* = 293 K.

References

1 B. Finkler, C. Spies, M. Vester, F. Walte, K. Omlor, I. Riemann, M. Zimmer, F. Stracke, M. Gerhards and G. Jung, *Photochem. Photobiol. Sci.*, 2014, **13**, 548-562.

2 P.Wang, L. Jullien, B. Valeur, J.-S. Filhol, J. Canceill, and J.-M. Lehn. *New J. Chem*., 1996, **20**, 895–907.

3 M. Emond, T. Le Saux, S. Maurin, J.-B. Baudin, R. Plasson, L. Jullien, *Chem. Eur. J*., 2010, **16**, 8822-8831.

4 P. Klán, T. Šolomek, C. G. Bochet, A. Blanc, R. Givens, M. Rubina, V. Popik, A. Kostikov and J. Wirz, *Chem. Rev.*, 2013, **113**, 119-191.

5 M. Digman, C. Brown, P. Sengupta, P. Wiseman, A. Horwitz, and E. Gratton. *Biophys. J.*, 2005, **89**, 1317–1327.

6 C. Brown, R. Dalal, B. Hebert, M. Digman, A. Horwitz, and E. Gratton. *J. Microsc.*, 2008, **229**, 78–91.